The Small Dispersion Limit for a Nonlinear Semidiscrete System of Equations

By Cristina Vilma Turner and Rodolfo Rubén Rosales

Numerical experiments that illustrate the emergence of oscillatory behavior in the solutions of a dispersive scheme approximating the Hopf equation are presented. The oscillations arise at the same time that the classical solution of the Hopf equation develops a singularity and generally have a spatial period equal to twice the grid size. Modulation equations for these period-two solutions are derived. The modulation equations have both a hyperbolic and an elliptic region. The period-two oscillations break down after they enter the elliptic region, and the solution blows up. We give a local description of the blowup by an exact solution. This kind of phenomenon (the blowup) has not been observed for integrable schemes. The modulation equations also have the unusual feature that they admit (some) shocks when crossings of characteristics in the hyperbolic regime occur. Other crossings lead to breakdown of the binary oscillation description, with oscillatory behavior of a more complicated nature arising.

1. Introduction

In this article, we examine the large oscillations arising in a dispersive semidiscrete approximation to the Hopf equation initial value problem for

Address for correspondence: Professor Rodolfo Rubén Rosales, Department of Mathematics, Room 2-337, Massachusetts Institute of Technology, Cambridge, MA 02139.

STUDIES IN APPLIED MATHEMATICS 99:205–254

Published by Blackwell Publishers, 350 Main Street, Malden, MA 02148, USA, and 108 Cowley Road, Oxford, OX4 1JF, UK.

$u = u(x,t)$,

$$\begin{aligned} u_t + (u^2)_x &= 0, \\ u(x,0) &= f(x), \end{aligned} \tag{1.1}$$

where $f = f(x)$ will (generally) be smooth. Various (appropriate) boundary conditions will be used to limit x to a finite interval.

The approximation we consider is given by the following semidiscrete (continuous in time, discrete in space) dispersive difference scheme

$$\dot{u}_n + \frac{1}{2h}\left(u_{n+1}^2 - u_{n-1}^2\right) = 0, \tag{1.2}$$

where n is an integer index, $0 < h \ll 1$, $u_n = u_n(t)$ and the dot indicates the time derivative: $\dot{u}_n = (d/dt)u_n$. The interpretation is that a spatial grid, $x_n = nh + x_0$, with uniform spatial grid size h, has been introduced. Then $u_n(t) \approx u(x_n,t)$ and $(u^2)_x$ in (1.1) is replaced by a centered difference quotient.

Initial conditions for (1.2), consistent with the discretization above and (1.1), are given by

$$u_n(0) = f(x_n) \qquad \text{for } x_n = nh + x_0, \tag{1.3}$$

where x_0 is some arbitrary fixed constant. Various (appropriate) boundary conditions are used to restrict n in (1.2) to a finite range—say $0 < n < N$, corresponding to $x_0 \le x \le x_0 + Nh$ in (1.1). Then the limit $h \to 0$, $Nh =$ constant is considered for the solutions of (1.2)–(1.3).

The rest of this introductory section is organized as follows: First, in Section 1.1, we give some motivation and background on a related problem. Next, in Section 1.2, we introduce the general kind of questions that motivate us and form the background for our ongoing research effort, which we start reporting in this article. Third, in Section 1.3, we explain how the problem (1.2)–(1.3) and the limit $h \to 0$ fits in the context of the general problem described in Section 1.2. Next, in Section 1.4, we relate our research to work by other on schemes similar to (1.2). Finally, in Section 1.5, we conclude with a description of the contents and results in the rest of the article.

1.1. Motivation and background

Assume in (1.2) that $u_n(t) = u(x_n,t)$ for some smooth $u = u(x,t)$, as (1.2) presumes as an approximation to (1.1). Then expanding $u_{n\pm1}$ in a Taylor series centered at x_n, the leading-order truncation error for the scheme (1.2)

is found to be

$$u_t + (u^2)_x + h^2\left(\frac{1}{6}u^2\right)_{xxx} = O(h^4). \tag{1.4}$$

It follows then that the continuum limit ($h \to 0$) of (1.2) should present many similarities with the well-understood zero dispersion limit ($\epsilon \to 0$) for the Korteweg–de Vries initial value problem

$$\begin{aligned} u_t + (u^2)_x + \epsilon^2 u_{xxx} &= 0, \\ u(x,0) &= f(x). \end{aligned} \tag{1.5}$$

This problem has been studied by Lax and Levermore [1] and Venakides [2]. A very complete review of the state of the field for this and related problems was done by Lax et al. in [3]. For the sake of completeness we briefly enunciate the results in [1, 2] for the behavior of the solution $u = u(x,t;\epsilon)$ of (1.5) in the limit $\epsilon \to 0$.

(i) As long as the problem (1.1) has a smooth solution $u = u(x,t)$, then the solution to (1.5)—with the same initial data—converges uniformly to $u(x,t)$, as $\epsilon \to 0$. In fact, it is well known that the classical solution of the Hopf initial value problem (1.1) ceases to exist and develops an infinite derivative after a finite time t_0, for any initial data with a decreasing part, even if the data are smooth. But, as long as this solution remains classical, a Strang-type convergence theorem [4] assures us that the solution of (1.5) (respectively (1.2)–(1.3)) converges strongly to it as $\epsilon \to 0$ (respectively $h \to 0$).

(ii) For $t > t_0$, the breakdown time for the solution of (1.1), $u(x,t;\epsilon)$ develops oscillations of $O(1)$ amplitude and $O(\epsilon)$ wavelength. If $x - x_0$ is the space location where the infinite derivatives for the solution of (1.1) occur when $t = t_0$, then the oscillations in $u(x,t;\epsilon)$ start there, on $x = x_0$, and spread in time over a spatial interval of length $O(t - t_0)$. Thus, for $t > t_0$, the limit $\epsilon \to 0$ of $u(x,t;\epsilon)$ exists only in the weak sense.

(iii) For t immediately after t_0 the oscillations in the solution $u = u(x,t;\epsilon)$ can be described in terms of a modulated *single-phase* solution of (1.5)—a traveling wave solution of the Korteweg–de Vries equation (1.5), $u = U(\theta)$, where U is a 2π-periodic function of θ and $\theta = (kx - \omega t)/\epsilon$. The single-phase solutions of (1.5) can be characterized by three independent parameters, for example: mean value β, amplitude A, and wave number k. The wave frequency is then given in terms of these by a dispersion relation $\omega = \omega(\beta, A, k)$ (see [5]). Then the modulation equations are a set of (hyperbolic) equations describing the evolution of these parameters over

space–time scales (x,t) much larger than those of $O(\epsilon)$ given by θ. These equations include the description in (i) since: When $A \equiv 0$, β satisfies the Hopf equation and k becomes a "ghost" variable, with no meaning for u.

(iv) The description in terms of a single-phase solution may eventually break down, as the modulation equations are nonlinear hyperbolic and will (when their characteristics converge) develop infinite derivatives.[1] Then the description of $u = u(x,t;\epsilon)$ past this second time of breakdown, $t = t_1$, requires the modulation equations for two phases (with five independent parameters), also hyperbolic. This process can repeat itself again and again, with a new phase (and two new parameters) appearing (generally) at each wave breakdown by converging characteristics of the modulation equations at the prior level of complexity.

The description of the limit $\epsilon \to 0$ of (1.5) thus requires the use of the modulation equations for n-phases $(n = 0, 1, 2\ldots)$[2] involving $(2n+1)$ hyperbolic equations in $(2n+1)$ variables (e.g., n amplitudes, n wave numbers and the mean level, although this is not the best set of variables to use). The weak limit $\bar{u}$ of the solution of (1.5) as $\epsilon \to 0$ was first studied by Lax and Levermore in [1]. Their description of the limit is in terms of a neat quadratic minimization problem subjected to inequality side conditions. They cleverly show that the solution of this minimization problem is equivalent to an expression for $\bar{u}$ in terms of $(2n+1)$ parameters[3] that satisfy a set of nonlinear hyperbolic equations, which turn out to be the modulation equations. Venakides [2], in a very thorough set of papers, completed the picture outlined in (i) through (iv) above. Further relevant work was done by McLaughlin and Strain [6], Tian [7], and Wright [8]. The question of what are the n-phase modulation equations for the Korteweg–de Vries equation was considered directly (independently of any connection with a small dispersion limit) by Flaschka et al. in [9].

1.2. *Statement of the general problem*

The work just described depends crucially on the fact that the Korteweg–de Vries equation is completely integrable, with an associated inverse spectral transform (see [10]) that allows for the general solution to be written exactly, at least in principle. For more general nonlinear dispersive systems, even though the analogs of (i) through (iii) above may still make sense (and be true), (iv) will not even be meaningful. This is because then

[1] Also: if the Hopf equation (as in (i)) breaks down at two different locations, two (expanding) oscillatory regions (described by (iii)) will develop. If these regions "collide," a breakdown occurs. Since in fact the Hopf equation is included in the modulation equations mentioned in (iii) as a special limit, this is actually not a different case.

[2] The case $n = 0$ corresponds to the Hopf equation: mean level only.

[3] For some integer n that may change in time.

even the meaning of a multiple-phase wave solution is rather unclear—and attempts to tackle the question by small amplitude expansions lead to *small divisors* problems. One may wonder then how much of the "orderly" fashion in which new phases appear for equations such as (1.5) depends on their integrability and how much reflects the "general" behavior of weakly dispersive nonlinear systems. In fact, one should even wonder if the notion of "phase" itself is an appropriate tool/concept in this context, or just a peculiarity of integrable systems.

To be more specific, for continuous (governed by p.d.e.'s) dispersive systems, a fairly general modulation theory for single-phase waves[4] can be formulated (see [5]). But the equations of this theory seldom allow solutions to exist for all times, even with smooth initial data. A frequent difficulty is that, because the equations are nonlinear hyperbolic they develop infinite derivatives in the solution (by crossing of characteristics) after a finite time. A second difficulty is that the equations may change type[5] (becoming elliptic). Natural questions one may ask are then:

(v) What happens with the solution to the dispersive system that the modulated wave describes after the breakdown of the modulation equations?

(vi) Can we describe the evolution of this solution, past the breakdown time, in some way that involves only "global" parameters, without need to follow the details of each oscillation in the solution?

(vii) Elaborating more on (vi): Is there some more general theory than modulation theory—as presented in [5], say—that would be able to carry us beyond the breakdown times?

When the breakdown occurs because of the crossing of characteristics in the modulation equations, then it is natural to interpret this as having waves[6] (that were separated in space initially) converging into the same region of space. This suggests that a multiple-phase region ought to develop, which agrees with the behavior of (1.5), as described above. This simple picture is complicated, for nonlinear dispersive systems,[7] by several factors:

(viii) The waves interact. Thus, once two or more waves converge into a region of space, new "objects" may be generated. Then these interact back with the original waves, and so on. There is no telling where the process may

[4] It is crucial for this theory that the notion of a periodic plane steady traveling wave has a clear meaning in this case.

[5] This is related to the underlying modulated periodic plane steady wave becoming unstable. Then the notion of a slowly varying periodic plane wave ceases to make sense and modulation theory breaks down. Whatever happens afterward is unlikely to be modelizable by a modulation "type" theory.

[6] Each with its own phase, amplitude, etc.

[7] For linear systems the simple picture applies.

end. This is illustrated by the difficulty in giving a clear meaning to the notion of a "multiple-phase" wave for general nonlinear dispersive systems, mentioned before.

(ix) Waves can be generated out of "nowhere." This is illustrated by the situation in Equation (1.5) (see (ii) above) where the breakdown for the Hopf equation leads to oscillations that were not present initially.

In any event, after a breakdown of this kind, we generally expect the solution to remain "oscillatory"—in particular with a weak limit (only) as the dispersion vanishes ("zero dispersion limit"). In this case something like (vii) seems like a reasonable hope, even if "hard." On the other hand, when the breakdown is due to the modulation equations becoming elliptic, violent departures from the "simple" picture provided by modulation theory may occur and then (vii) is probably too much to expect—at least with any degree of generality.

We note that for continuous nonlinear dispersive systems that allow arbitrary "mean values" in their periodic plane traveling waves (e.g., the Korteweg–de Vries equation, (1.5)) one can consider "zero-phase" modulations. As these equations break down, in many cases the problem should be tractable within the context of the general theory in [5]—with the breakdown signifying that a single phase is generated.[8] This issue was first explored by Gurevich and Pitaevskii in [11], for the particular case of the Korteweg–de Vries equation (using the general theory in [5], not the inverse spectral transform). A general analysis seems lacking, possibly due to the fact that the modulation equations, as given by the theory in [5], can be quite complicated—except in the "near-linear" regime.

Finally, we remark that this limiting behavior of nonlinear dispersive systems contrasts sharply with that for solutions of any zero dissipation limit; for instance the limit as $\epsilon \to 0$ of the Burgers equation

$$u_t + (u^2)_x - \epsilon^2 u_{xx} = 0. \tag{1.6}$$

In this case the solution converges almost everywhere and strongly to a weak solution of (1.1) with shock discontinuities.

1.3. Plan of attack

The questions posed in the prior subsection are clearly very hard.[9] Further, there may be more than one answer, as a definition by negation of the systems involved (noncompletely integrable...) is far too broad and vague to

[8] In other words, (i), (ii), and (iii) before are fairly general behavior. It is only (iv) that is peculiar to integrable systems.

[9] Thus to expect any prompt resolution of them seems unreasonable. A good deal of modesty in approaching these questions seems appropriate.

guarantee a precise answer. As our knowledge and intuition concerning the possible behaviors that can be expected seems quite limited, a good first approach should (we review prior work by others on this in Section 1.4)

(x) begin the study with the simplest types of equations that seem to have the "desired" properties,

(xi) include a lot of careful numerical studies, to explore and classify possible (interesting) behaviors—while pushing our current analytical understanding as far as possible, in an "interactive" fashion.

Concerning (xi), we remark that numerical experiments that are too far removed from any theoretical basis of understanding can easily be meaningless. One learns best when it is possible to jump back and forth between theory and experiment, and we have tried to follow this method.

The simplest nonlinear dispersive systems are probably those that reduce to the Hopf equation (1.1) when the zero dispersion limit is taken " naively." On the other hand, semidiscrete systems are easier to integrate numerically than continuous ones. Thus it would seem that a good choice as far as (x) and (xi) above should be some kind of dispersive discretization of the Hopf equation. Of the very many possible ones, the two simplest seem to be (1.2) and[10]

$$\dot{u}_n + \frac{1}{n} u_n (u_{n+1} - u_{n-1}) = 0. \tag{1.7}$$

But this second scheme is "completely integrable" (as explained later in Section 1.4) and thus "too special." On the other hand, (1.2) appears to be nonintegrable, although we have no proof of it (this is a question we plan to study further in later work).

It would seem that semidiscrete systems should be easier to analyze than continuous ones, but this is not entirely true—perhaps the price to be paid for simpler numerics? For example:

(xii) Even though—in principle—a general theory for single-phase wave modulation, similar to the one formulated in [5], should be possible for semidiscrete systems, this is not so. The problem is that the notion of a "periodic plane steady traveling wave" ceases to have a clear meaning for these systems.[11] For example, we have been unable to find any such waves for (1.2), except as small amplitude perturbation expansions.

(xiii) The solutions to problems such as (1.2) (1.3) have a *strong phase dependence*. Namely, if we write $x_n = \sigma h$ (with $0 \le \sigma \le 1$ fixed as $h \to 0$), the

[10] Note that one-sided differences yield dissipative schemes and so are not an option.

[11] Except in the completely integrable cases and other special examples (see [12] for a derivation and study of general modulation equations for semidiscrete nonlinear Schrödinger-type equations).

solutions for different values of σ can differ strongly. We illustrate this with numerical experiments and also provide analytical explanations.

(xiv) Because of their discreteness, systems like (1.2) may admit (in the limit $h \to 0$) discontinuous behavior across certain values of x; i.e., the nature of the limit behavior changes abruptly at some point. This means (in particular) that shocks may be admissible in the solutions to the modulation equations. We note that this is less a product of the discreteness than of the fact that the dispersion is nonlinear.[12] Again, we illustrate this with both numerical examples and theory.

Going now back to (1.2)–(1.3) and the analogy with (1.5) via (1.4): After the breakdown time for the classical solution to (1.1), we expect the solution of (1.2) to develop oscillations at the grid level—wavelength of order h—of nonvanishing amplitude. Thus, after the breakdown time the solution can (at best) be expected to have a limit as $h \to 0$ only in the weak sense. Using bars to denote weak limits

$$\bar{u}_t + \left(\overline{u^2}\right)_x = 0. \tag{1.8}$$

But, since $(\overline{u^2}) \neq (\bar{u})^2$, (1.8) is not enough to determine $\bar{u}$. The "general problem" we posed before in Section 1.2 can now be restated (for the particular case of (1.2)–(1.3)) as: **Find enough information about the solution and the limit $h \to 0$, to "close" (1.8).** This entails finding which other parameters, in addition to $\bar{u}$, control and completely determine the time evolution of the weak limit—and then writing the evolution equations for these parameters.

The analogy between (1.4) and (1.5) should not be pushed too far, as the dispersion term in (1.4) is nonlinear—which can cause dramatic differences in behavior. For example, the solutions of (1.5) are generally smooth, but this is not so for (1.4)—see (xiv) above and [13]. The same can be said of the relationship between (1.2) and (1.4). When oscillations with wavelength of order h and finite amplitude develop in (1.2), it is no longer valid to neglect in (1.4) the right-hand side term.

1.4. Related prior work

Here we briefly summarize related work by other researchers on semidiscrete dispersive systems. A complete and thorough review (by Lax et al.) can be found in [3].

[12] For example, consider Equation (1.4), with the right-hand side set to zero. The resulting (dispersive) p.d.e. admits solutions with stationary "shocks," where u^2 is smooth across the discontinuity—but u changes sign.

Only two (integrable) semidiscrete schemes have been carefully studied and they are essentially identical. One of them is the Toda lattice[13] (see [14, 15])

$$\dot{a}_n = \frac{1}{h} a_n (b_{n+1} - b_n) \qquad \text{and} \qquad \dot{b}_n = \frac{2}{h}\left(a_n^2 - a_{n-1}^2\right), \tag{1.9}$$

or (alternatively)

$$\ddot{q}_n + \frac{1}{h}\left\{\exp\left[-\frac{q_{n+1} - q_n}{h}\right] - \exp\left[-\frac{q_n - q_{n-1}}{h}\right]\right\} = 0, \tag{1.10}$$

where $a_n = \frac{1}{2}\exp[-(1/2h)(q_n - q_{n-1})]$ and $b_n = -\frac{1}{2}\dot{q}_{n-1}$. The other, introduced by Kac and van Moerbeke in [16], is

$$\dot{p}_n + \frac{1}{2h} p_n \left(p_{n+1}^2 - p_{n-1}^2\right) = 0. \tag{1.11}$$

Their equivalence was shown by Moser in [17].

Holian et al. [18] studied the Toda Lattice with step (shock) initial conditions and discovered that period-two oscillations were generated. This seems to be a common feature to all semidiscrete systems currently in the literature.[14] Venakides et al. [19] analyzed the problem using the inverse spectral transform machinery and reconfirmed the results in [18], in particular the generation of period-two oscillations.

Goodman and Lax[15] [20] studied (1.7), with initial conditions as in (1.3), very much in the same spirit we study here (1.2). However, (1.7) is also integrable,[16] as for $u_n > 0$ the transformation $u_n = p_n^2$ reduces it to (1.11). Hou and Lax [22] studied a dispersive discretization of the Euler equations of gas dynamics with initial conditions as in (1.3). Finally, Levermore and Liu [23] studied the scheme (also a discretization of (1.1))

$$\dot{u}_n + \frac{1}{3h}(u_{n+1} + u_n + u_{n-1})(u_{n+1} - u_{n-1}) = 0 \tag{1.12}$$

with initial conditions as in (1.3). All these studies show the formation of (mostly) period-two oscillations right after the breakdown time for the Hopf equation (or gas dynamics for [22]). In [23] a breakdown by the period-two modulation equations changing type to elliptic is also found.

---

[13] We introduce here the parameter h, not present in the original references, for the sake of consistency with (1.2). Clearly this only amounts to a simple rescaling of time.

[14] Currently we are studying a system for which this is not true, as period-three oscillations arise.

[15] There is a factor of 2 difference between (1.7) and the scheme used in [20]. We introduce this time scale change here so that (1.7) is consistent with (1.1).

[16] In fact, Hayes [21] has recently studied this scheme and found a large class of very interesting relevant exact solutions — although he did not use an inverse spectral transform approach for this.

The oscillatory nature of the solutions of dispersive difference schemes was discovered by von Neumann in 1944—in a calculation of compressible flows with shocks in one space dimension, using centered differences [24]. After shocks formed, oscillations on the mesh scale appeared. Von Neumann suggested that the oscillations should be interpreted as heat energy produced by the irreversible action of the shock wave and conjectured that (as $h \to 0$ and $dt \to 0$) the solutions of the difference equations would converge (weakly) to the exact (discontinuous) solution of the equations governing the compressible fluid.[17] The studies in [20, 22, 23] appear to have been motivated, at least partly, by this conjecture. Their results show that there is good reason to doubt the validity of von Neumann's conjecture.

Finally, we should mention here the pioneering work of Fermi et al. [25], which (even though not directly concerned with the problems of interest here) showed that very many interesting and unexpected behaviors can occur in nonlinear lattices. A continuum (completely integrable) system whose small dispersion limit has also been studied is the nonlinear Schrödinger equation; see [26, 27].

The scheme that we study here, (1.2), allows for a large variety of shocks in the modulation equations, a new and interesting feature that the schemes studied by other researchers do not permit. This allows for the occurrence of some very interesting behaviors, not observed before, which will be reported and analyzed here and in another publication in preparation.

1.5. Plan of the paper

In this article we emphasize the numerical aspects of what we have learned so far about the behavior of the problem (1.2)–(1.3). We concentrate on the more analytic aspects of our study in a later publication, in particular on the details of the shock conditions for the modulation equations and how they depend on the phase x_0 in the initial conditions (see (1.3) and (xiii)).

The rest of the article is organized as follows: In Section 2 we present a variational principle and conservation laws for the scheme. We introduce the period-two solutions, study their stability, and show that they admit "shocks." An explanation of why period-two solutions should be so important is given in terms of the potential needed in the Lagrangian formulation of the equations.

In Section 3 the modulation equations for binary oscillations are derived. Their characteristic forms and Riemann invariants are displayed, together with shock conditions for the shocks they allow. An exact analytical solution is obtained for the case of step initial data.

[17] For a detailed historical account of these facts, see [22].

In Section 4 numerical experiments showing the generation of period-two oscillations after the breakdown of the Hopf equation are shown. Comparisons with exact solutions of the modulation equations are also shown. Finally, examples showing the blowup of the solutions (of the scheme) once the modulation equations cross into the elliptic region are shown. A local description of the blowup for the scheme (in terms of an exact solution) is proposed.

In Section 5 the phase dependence of the solutions with binary oscillations is explored in several examples. Comparisons with exact solutions are shown. The phase dependence of the shocks in the modulation equations is studied (numerically) in some detail.

Finally, in Section 6, the production of oscillatory pulses by a shock moving slowly through the grid is illustrated. This gives rise to oscillations that are not binary and for which we have not been able to develop a precise characterization.

2. Variational principle, conservation laws, and period-two solutions

In this section we study some simple properties and solutions of the system of Equations (1.2) and compare them with the analog properties of the schemes (1.7) and (1.12)—studied, respectively, in [20, 23]. First we show that the system has a Lagrangian and explore the connection with modulation theory, as presented in [5]. We explain how the fact that the *potential* has two integration constants is related to the appearance of period-two oscillations. Next we look at the conserved quantities and note that the solutions to the system can develop singularities in a finite time. Finally, we examine the period-two solutions, their stability properties, and the fact that they admit "shocks."

2.1. Variational forms

For simplicity[18] consider now the scheme (1.2) on $-\infty < n < \infty$, with u_n vanishing (fast enough) as $|n| \to \infty$. First we note that, if we introduce a *potential* sequence $\{\Phi_n\}$ to $\{u_n\}$ by

$$u_n = \frac{1}{2h}(\Phi_{n+1} - \Phi_{n-1}), \tag{2.1}$$

then (1.2) follows from a *variational principle* with *Lagrangian*

$$L = \sum_{-\infty}^{\infty} \left(\frac{1}{2} \dot{\Phi}_n u_n + \frac{1}{3} u_n^3 \right). \tag{2.2}$$

[18] Similar results are valid in other cases, such as a periodic lattice, with $u_{n+N} = u_n, -\infty < n < \infty$, for some N. The extensions are obvious and we do not display them here.

Thus (1.2) is a discrete analog of the kind of systems for which the *Average Lagrangian* approach to modulation theory was developed by Whitham—see [5]. Unfortunately, we have not been able to find expressions for general plane steady traveling wave solutions of (1.2)—nor do we even know if such objects actually exist in any general sense for the scheme. Thus a general and powerful theory as that in [5] is not available to us here—this is the difficulty pointed out in (xii) of Section 1.3. Thus the analog of (iii) in Section 1.1 for problem (1.5) will not be complete for (1.2)–(1.3). In our numerical experiments we have found instances where (after the breakdown time for the Hopf equation) oscillations appear, but we have no good theory to model them; see the last experiment in Section 6. We do not yet know whether this is merely a technical difficulty or if something truly novel is involved in the behavior of (1.2)–(1.3) relative to that of (1.5) (in the limits $\epsilon, h \to 0$). We plan to investigate this matter in future work.

Remark 2.1: The potential sequence $\{\Phi_n\}$ is determined by $\{u_n\}$ from (2.1) up to *two* arbitrary constants

$$\Phi_n = c(n) + 2h \sum_{j=0}^{\infty} u_{n-2j-1}, \tag{2.3}$$

where $c(n) = \alpha$ if n is even and $c(n) = \beta$ if n is odd. This is rather unusual behavior if one thinks in terms of potentials for p.d.e.'s, but rather natural for discrete systems. It is one way to understand the ubiquitous occurrence of period-two oscillations for centered difference schemes as (1.2), as we explain now: Recall that in Whitham's Average Lagrangian theory [5], whenever a potential appears in the Lagrangian form of the dispersive system, a corresponding "pseudo-phase" must be introduced into the Average Lagrangian formulation. These are, in turn, associated with variable "mean levels" in the solution. In the case of the Korteweg–de Vries equation, for example, it is the modulation of the mean level that gives the Hopf equation—as in (i) of Section (1.1). For (2.2), however, one should introduce *two* pseudo-phases. When these two coincide, the Hopf equation follows; otherwise period-two oscillations arise.[19] One may say that an extra step between (i) and (ii) in Section 1.1 appears for systems like (1.2). Anyway, at this stage, this is all very speculative and much work remains to be done.

[19] Note that the constants in (2.3) are different for n odd or even. We elaborate more on this on Remark 3.1.

Remark 2.2: Introduce the skew-adjoint operator on sequences J, defined for any $\mathbf{u} = \{u_n\}$ by

$$(J\mathbf{u})_n = -\frac{1}{2h}(u_{n+1} - u_{n-1}), \qquad -\infty < n < \infty. \tag{2.4}$$

Then (1.2) has the generalized Hamiltonian form

$$\dot{\mathbf{u}} = J \operatorname{grad} H, \qquad H = \frac{1}{3}\sum_n u_n^3, \tag{2.5}$$

with Hamiltonian H. A classical Hamiltonian form follows if we note that Φ_n in (2.1) can be chosen so that

$$\dot{\Phi}_n = -u_n^2, \tag{2.6}$$

upon integration in (1.2). Thus, with $q_n = u_n$ and $p_n = \Phi_n$, the scheme is equivalent to the classical Hamiltonian system with Hamiltonian

$$\tilde{H} = \frac{1}{3}\sum\left\{q_n^3 + \frac{1}{8h^3}(p_{n+1} - p_{n-1})^3\right\}, \tag{2.7}$$

provided that the initial conditions are such that $q_n = (1/2h)(p_{n+1} - p_{n-1})$. This condition is then preserved by the flow.

Remark 2.3: The scheme (1.7), studied by Goodman and Lax in [20], also has a Lagrangian—at least for positive solutions. For example, let $u_n = \exp(v_n)$. Then (1.7) reduces to

$$\dot{v}_n + \frac{1}{h}(e^{v_{n+1}} - e^{v_{n-1}}) = 0. \tag{2.8}$$

Introducing the potential $v_n = (1/2h)(\Phi_{n+1} - \Phi_{n-1})$, this has the Lagrangian

$$L = \sum_{-\infty}^{\infty}\left(\frac{1}{2}\dot{\Phi}_n v_n + 2e^{v_n}\right), \tag{2.9}$$

where again two arbitrary constants appear in the potential.[20] Another Lagrangian is provided by the equivalence of the equations with the system (1.10)

$$L = \sum_{-\infty}^{\infty}\left[\frac{1}{2}\dot{q}_n^2 - \exp\left(-\frac{q_{n+1} - q_n}{h}\right)\right]. \tag{2.10}$$

[20] Written in the form (2.8), it is clear that this scheme also has a generalized Hamiltonian form, as in (2.4)—(2.5) but with $H = 2\Sigma_n e^{v_n}$.

Given that this scheme is completely integrable, it should be possible to produce a theory for the $h \to 0$ limit that does not differ too much—qualitatively—from that for the Korteweg–de Vries equation, as described in (i)–(iv) of Section 1.1.

Remark 2.4: We searched for a variational principle that would apply to the scheme (1.12), studied by Levermore and Liu [23], and were not successful—although our search was not thorough. It would be interesting to know if there is one and if it also involves a potential depending on two arbitrary constants.

2.2. *Conservation laws*

We have been able to find only two conservation laws for the scheme (1.2), namely, conservation of "mass" and the Hamiltonian in (2.5)

$$M = \sum_n u_n \qquad \text{and} \qquad H = \frac{1}{3}\sum_n u_n^3. \tag{2.11}$$

In fact, $M_e = \sum u_{2n}$ and $M_o = \sum u_{2n+1}$ are *conserved separately.*

None of these conserved quantities is enough to bound the growth of u_n—and in fact the solutions of (1.2) may blow up in a finite time. We contrast this behavior with that of the schemes studied previously. The scheme (1.12) conserves $E = \frac{1}{2}\sum_n u_n^2$, in addition to M, and this bounds the growth of the solutions. On the other hand, the scheme (1.7) keeps $u_n > 0$ for all n's (if this it true initially);[21] thus the conservation of M provides a bound on the growth of the solutions. By contrast, this "positivity" property is not true for (1.2)—as Example 2.1 below shows—and thus the conservation of M provides no bound.

EXAMPLE 2.1. Consider (1.2) with initial conditions: $u_n(0) = 2$ for $n > 0$, $u_n(0) = 1$ for $n < 0$, and $u_0(0) = \delta$, where $0 < \delta \ll 1$. Then $\dot{u}_0(0) = -3/2h$ and it is clear that u_0 must cross zero rather quickly. Furthermore, $\dot{u}_{-1}(0) \approx 1/h$, which causes $u_{-1}(0)$ to start growing (rapidly). This, in turn, causes $u_{-2}(0)$ to decrease—and so on. Thus, period-two oscillations appear for $n \le 0$. For $n > 0$ the same type of argument shows that all the u_n's start decreasing and no oscillations arise. We do not analyze the evolution of this solution for longer times. This example should give an intuitive idea of the mechanism that produces period-two oscillations in the solutions of (1.2).

[21] A simple proof can be done using that if $u_n > 0$ initially, then we can solve (2.8) with initial conditions $v_n(0) = \ln u_n(0)$. Since then $u_n = \exp(v_n)$, clearly $u_n > 0$ for all times (see [20]).

In our numerical experiments we observed many instances of a solution blowing up in finite time. These were almost always associated with the appearance of regions of period-two oscillations where the "same sign" condition on u_n was violated, producing growth in the amplitude of the oscillations in a very localized region of space, followed by a finite time localized blowup (see Section 4.3).

2.3. *Period two solutions — Stability*

A very simple exact solution of the Equations (1.2)[22] is that given by

$$u_{2n} = a \text{ and } u_{2n+1} = b \qquad \text{for } -\infty < n < \infty, \tag{2.12}$$

where a and b are arbitrary constants (in particular, $a = b$ yields the trivial solution $u_n \equiv$ const.). A linearized stability analysis of this solution yields

$$\dot{A}_n + \frac{b}{h}(B_{n+1} - B_{n-1}) = 0 \qquad \text{and} \qquad \dot{B}_n + \frac{a}{h}(A_{n+1} - A_{n-1}) = 0, \tag{2.13}$$

where $u_n = a + A_n$ for n even and $u_n = b + B_n$ for n odd. Thus, if we write

$$A_n = \alpha(t) r^n \qquad \text{and} \qquad B_n = \beta(t) r^n, \tag{2.14}$$

where $r = e^{ik}$, we obtain

$$\dot{\alpha} + 2i\frac{b}{h}(\sin k)\beta = \dot{\beta} + 2i\frac{a}{h}(\sin k)\alpha = 0. \tag{2.15}$$

We conclude that

1. the solution (2.12) is linearly stable (respectively unstable) for $ab > 0$ (respectively $ab < 0$) and
2. when $ab = 0$, *but* $a^2 + b^2 > 0$, then either α of β in (2.15) will grow linearly in time.

The instability when $ab < 0$ is related to the fact that the period-two modulation equations become elliptic; see Section 3.2. Our numerical experiments show that, once the instability is triggered, it causes blowup of the solution in a finite time. A similar phenomenon (of instability of the period-two oscillations and ellipticity in the modulation equations) occurs for the system (1.12), except that there no blowup can occur as $E = \frac{1}{2}\Sigma u_n^2$ is

[22] Also, of (1.7) and (1.12).

conserved. The numerical experiments in [23] show rather complicated behavior in the breakdown region. Finally, because (1.7) preserves the positivity of the solutions, this type of instability appears irrelevant, as no evolution from the hyperbolic to the elliptic regime (in the period-two modulation equations) is possible.

2.4. Period two solutions — Shocks

It is rather interesting to observe that we can switch the sign in (2.12) at any arbitrary place (for any a and b) and u_n will remain a solution of (1.2). Namely, we can take u_n given by (2.12) for $n \le n_0$—some n_0—and by (2.12) with (a, b) replaced by $(-a, -b)$ for $n > n_0$. The existence of these solutions with switches translates into the period-two modulation equations accepting steady-state shocks with the appropriate jump conditions. This is rather unusual behavior for modulation equations.

Remark 2.5: In contrast, we note that the schemes (1.7) and (1.12) admit solutions with sign switches as above only if either a or b vanish, with $u_{n_0} = 0$ (where n_0 is the switchover point, as above). Because of this difference, the problem (1.2)–(1.3) exhibits interesting behaviors (related to shocks in the weak limit) that are not present in the other schemes. We illustrate this in what follows.

3. The modulation equations for binary oscillations

In this section we derive the modulation equations for binary oscillations—which include the Hopf equation as a special subcase—and start their analysis. We study where these equations are hyperbolic and elliptic and find their Riemann invariant form in the hyperbolic case. Finally we consider steady-state shocks for the equations. We show that the Rankine–Hugoniot jump conditions are not enough to determine the solution and introduce an extra equation to close the system. An exact analytical solution is then provided for the case of step initial data.

3.1. Asymptotic expansion

We note that the scheme (1.2) can be split into two "sub-schemes." Namely—compare this with (2.12)—introduce $\{A_n\}$ and $\{B_n\}$, defined only for n even and odd, respectively, by

$$u_n = A_n \text{ for } n \text{ even} \qquad \text{and} \qquad u_n = B_n \text{ for } n \text{ odd}. \tag{3.1}$$

Then we have the equations

$$\dot{A}_n + \frac{1}{2h}\left(B_{n+1}^2 - B_{n-1}^2\right) = 0 \qquad \text{and} \qquad \dot{B}_n + \frac{1}{2h}\left(A_{n+1}^2 - A_{n-1}^2\right) = 0. \tag{3.2}$$

We now propose an asymptotic expansion for solutions of these equations, valid as $h \to 0$, of the form

$$A_n(t) \sim \sum_{m=0}^{\infty} h^m a_m(x_n,t) \qquad \text{and} \qquad B_n(t) \sim \sum_{m=0}^{\infty} h^m b_m(x_n,t), \tag{3.3}$$

where the x_n's are defined in (1.3) and the $a_m = a_m(x,t)$ and $b_m = b_m(x,t)$ are smooth functions of x and t. In particular, we consider the case $a_m = b_m = U_m(x,t)$, which is consistent with the initial conditions (1.3). Substituting into (3.2) (expanding in Taylor series around x_n any function evaluated at x_{n+1}) and collecting powers of h we obtain (at leading order)

$$a_t + (b^2)_x = 0 \qquad \text{and} \qquad b_t + (a^2)_x = 0, \tag{3.4}$$

where we have not written the subscript 0. In the particular case when $a = b = U$, this reduces to the Hopf equation

$$U_t + (U^2)_x = 0. \tag{3.5}$$

To this we must attach appropriate boundary conditions and the initial conditions

$$U(x,0) = a(x,0) = b(x,0) = f(x), \tag{3.6}$$

as follows from (1.3), (3.1), and (3.3).

Remark 3.1: If we use the variational approach to modulation, as in [5], we must split the potential Φ_n in (2.1) into two parts—as (2.3) shows we should—

$$\zeta_n = \Phi_n \text{ for } n \text{ odd} \qquad \text{and} \qquad \xi_n = \Phi_n \text{ for } n \text{ even}. \tag{3.7}$$

Approximating then ζ and ξ in the same fashion as (3.3), then from (2.1) we obtain—at leading order—

$$a = \zeta_x \qquad \text{and} \qquad b = \xi_x. \tag{3.8}$$

It follows then easily, from (2.2), that the appropriate Average Lagrangian is

$$\mathscr{L} = \frac{1}{2}(\dot{\xi} b + \dot{\xi} a) + \frac{1}{3}(a^3 + b^3), \tag{3.9}$$

where (3.8) should be used for a and b when calculating the variational equations. This, again, yields (3.4).

Remark 3.2: Given (3.4), the fact that a and b are equal initially—as in (3.6)—and that they satisfy the same boundary conditions (at least as far as it concerns the type of problems considered here), one may wonder how it ever develops that $a \neq b$. We see later (in Section 3.3) that this occurs because of conditions at the shocks—which happen to be strongly phase dependent. This is rather different from the situation for the problem in (1.5). In (1.5) (see (ii) and (iii) of Section 1.1), as oscillations develop after the breakdown of the Hopf equation approximation, an expansion fan appears in the one-phase modulation equations[23]—and no crossing of characteristics or shocks occur. Thus we see again, from a different but related point of view to that in Remark 2.1, that the occurrence of binary oscillations is intimately tied up to the discreteness of the system and that it is (probably) qualitatively distinct from the oscillations described in (ii) and (iii) of Section 1.1.

3.2. *Characteristics, invariants and change of type*

It is easy to see that the characteristic speeds for (3.4) are given by $\lambda_\pm = \pm 2\sqrt{ab}$. Thus the system is

$$\begin{array}{ll} \text{hyperbolic in the region} & ab > 0, \\ \text{elliptic in the region} & ab < 0. \end{array} \tag{3.10}$$

In particular, in the hyperbolic region $ab > 0$, (3.4) can be written in the **Riemann Invariant** form,

$$\frac{d}{dt}R = 0 \quad \text{along} \quad \frac{d}{dt}x = \nu\lambda \qquad \text{and} \qquad \frac{d}{dt}S = 0 \quad \text{along} \quad \frac{d}{dt}x = -\nu\lambda, \tag{3.11}$$

where $\nu = \pm 1 = \text{sign}(a) = \text{sign}(b)$, $R = |a|^{1.5} + |b|^{1.5}$, $S = |a|^{1.5} - |b|^{1.5}$ and $\lambda = 2\sqrt{ab} > 0$.

In our numerical experiments with solutions of (1.2) we often observed modulated binary oscillations in the hyperbolic regime that eventually evolved into the elliptic regime in a small region somewhere in space. When

[23] This mechanism was discovered in [11].

this happens the period-two oscillations become unstable—see Section 2.3—and, typically, explosive growth occurs afterward (with a very localized infinity developing in a finite time), as we illustrate in Section 4.3. This behavior is rather different from that reported for (1.12) in [23] after an elliptic breakdown occurs, while (1.7) never crosses into the elliptic region if the initial data are positive.

3.3. *Steady-state shocks*

From Section 2.4, it is clear that it is admissible to introduce into the solutions of (3.4) steady-state shocks. That is, we can have a discontinuity in the solution at some fixed $x = x_s$. Then, if $a_\pm$ and $b_\pm$ denote the values of the solution immediately ahead (+) and behind (−) of x_s, the conditions

$$a_+ = -a_- \qquad \text{and} \qquad b_+ = -b_- \tag{3.12}$$

must be satisfied.[24] If we interpret (3.4) as a pair of hyperbolic conservation laws, then (3.12) are precisely the appropriate Rankine–Hugoniot jump conditions for a stationary shock. This interpretation is consistent with the fact that the scheme (1.2) conserves both $M_e = \Sigma u_{2n}$ and $M_o = \Sigma u_{2n+1}$, as follows easily from (3.1) and (3.2) and pointed out in (2.11).

Remark 3.3: As follows from Remark 2.5, for the schemes (1.7) and (1.12), (3.12) should be augmented by $a_+ = 0$ or $b_+ = 0$.

Remark 3.4: It is important to note the interesting fact that (3.12) is not enough to determine the solution,[25] and one extra condition is needed. The numerical examples later will make this need abundantly clear but, to illustrate the point, consider the following:

EXAMPLE 3.1. Find the solution to the system of equations (3.4) for $t > 0$ on $-\infty < x < 0$ with initial and boundary conditions

$$a(x,0) = b(x,0) = 1 \qquad \text{and} \qquad b(0,t) = \alpha a(0,t), \tag{3.13}$$

where $0 \le \alpha \le 1$. We note that the case $\alpha > 1$ can be reduced to this one by exchanging the roles of a and b.

This problem is easy to solve, exactly, using (3.11). We note that $R = 2$ and so we have a *simple wave* in S, that then satisfies the single equation

$$S_t - \lambda S_x = 0, \qquad \lambda = 2\left(\frac{4 - S^2}{4}\right)^{1/3} \tag{3.14}$$

[24] Note that $a_+ b_+ = a_- b_-$, so no change of type occurs.

[25] In particular, the Lax "entropy" condition [28] is not satisfied. This condition would require here only one characteristic leaving the shock instead of two.

with

$$S(x,0) = 0 \text{ and } S(0,t) = 2\left(\frac{1-\alpha^{1.5}}{1+\alpha^{1.5}}\right).$$

Thus

$$\begin{aligned} S &= 0 \qquad \text{for } x \le -2t, \\ S &= 2\sqrt{1+\frac{x^3}{8t^3}} \qquad \text{for } -2t \le x \le -v(\alpha)t \\ S &= 2\left(\frac{1-\alpha^{1.5}}{1+\alpha^{1.5}}\right) \qquad \text{for } -v(\alpha)t \le x \le 0, \end{aligned} \tag{3.15}$$

where

$$v(\alpha) = 2\left[\frac{4\alpha^{1.5}}{(1+\alpha^{1.5})^2}\right]^{1/3}.$$

The second formula follows from an expansion fan starting at the origin that yields $\lambda = -x/t$. Thus we arrive at the following solution for Example 3.1, written in terms of a and b:

$$\begin{aligned} &a = b = 1 \qquad \text{for } x \le -2t, \\ &a = \left(1+\sqrt{1+\left(\frac{x}{2t}\right)^3}\right)^{2/3} \text{ and } \quad b = \left(1-\sqrt{1+\left(\frac{x}{2t}\right)^3}\right)^{2/3} \\ &\text{for } -2t \le x \le -v(\alpha)t \\ &a = \left(\frac{2}{1+\alpha^{1.5}}\right)^{2/3} \text{ and } b = \left(\frac{2\alpha^{1.5}}{1+\alpha^{1.5}}\right)^{2/3} \text{ for } -v(\alpha)t \le x \le 0. \end{aligned} \tag{3.16}$$

Now, take these functions a and b and extend them to the whole line $-\infty < x < \infty$, as odd functions. Then they solve (3.4) on $-\infty < x < \infty$ and $t > 0$ with initial conditions

$$a = b = 1 \ (\textit{for } x < 0), \qquad a = b = -1 \ (\textit{for } x > 0) \tag{3.17}$$

and a shock at $x = 0$ satisfying (3.12). But α can be taken arbitrary! This illustrates the point made in Remark 3.4 above. We note that the same arguments above would apply[26] to any odd initial condition in $-\infty < x < \infty$ for $a(x,0) = b(x,0)$ that breaks and forms a steady shock at $x = 0$ (e.g., $-\tanh x$).

[26] Except, of course, for the ability to produce an exact solution.

Remark 3.5: In the example above note that the oscillations generated at the shock (difference between a and b) go from a maximum for $\alpha = 0$ to none for $\alpha = 1$. When $\alpha = 0$, $v(\alpha) = 0$ and the oscillations decrease, as x decreases, from a maximum amplitude at $x = 0$ (where $a = 2^{2/3}$ and $b = 0$) to none along $x = -2t$ (where $a = b = 1$). When $\alpha = 1$, $v = 2$, and $a = b = 1$ everywhere, i.e., (3.5) applies. Of these solutions, the only one that has an analog in the modulation equations for binary oscillations in the schemes (1.7) and (1.12) is the one for $\alpha = 0$; see Remark 3.3.

Remark 3.6: From the considerations above, it follows that (3.12) must be augmented by one extra condition. In this article we use the ad hoc condition (as in (3.13))

$$b_\perp = \alpha a_\perp, \tag{3.18}$$

where $0 \le \alpha \le 1$ is given. In the numerical experiments where binary oscillations with a stationary shock appear (see Section 5) we can measure α. If then this measured α is used to integrate (3.4), (3.12), and (3.18), we find that the modulation equations reproduce the behavior of the solution of the scheme (1.2) as $h \to 0$ very well. We see that α in (3.18) depends, for a given fixed initial condition $f(x)$ in (1.3), on x_0. Typically, as x_0 ranges over an interval of width h (e.g., $x_0 = \sigma h, 0 \le \sigma \le 1$), α moves over the whole of $0 \le \alpha \le 1$. This, of course, means that the *behavior of the solution of (1.2)–(1.3) changes dramatically with small phase shifts* x_0.

In this article, we do not justify (3.18)—except for the cases when $\alpha = 0$ or $\alpha = 1$, where simple symmetry arguments can be used (see Section 4.1). A detailed theoretical analysis will be presented in a later publication. It turns out that (3.18) is a gross simplification of the actual conditions, which are quite subtle and interesting as they require the solution of "second-order" quantities in the approximation (3.3).

4. Some numerical experiments

In this section we consider various initial data for the problem (1.2)–(1.3) and integrate the equations numerically. The aim is to investigate what happens with the solution of the dispersive system (1.2)–(1.3) after the corresponding solution of the "long wave" approximation[27] (1.1)—the Hopf equation—breaks down.

We solve the system of Equations (1.2) using a code based on variable order, variable step Adam's methods. The code is completely documented and explained in [29]. (We express our gratitude to L. N. Trefethen, who made a version of the code available to us.)

[27] We call this approximation "long wave" because it applies when u_n depends very slowly on n, as in (3.3) with $a_m = b_m = U_m$.

We computed approximate weak limits (as $h \to 0$) from the numerical solutions by taking averages over adjacent spatial points with the formula

$$\bar{u}_n = \frac{1}{2M}\left(\frac{1}{2}u_{n-M} + \sum_{j=n-M+1}^{n+M-1} u_j + \frac{1}{2}u_{n+M}\right), \tag{4.1}$$

where $1 \ll M \ll 1/h$, for example, $M \approx 1/\sqrt{h}$. This same formula, with $M = 1$, was used to remove the period-two "component" from the solutions. When the solution is a modulated binary oscillation, $M = 1$ should give the same result as $M = O(1/\sqrt{h})$.

The rest of this section is organized into the following subsections: In Section 4.1 we present experiments with sinusoidal initial conditions, which break at time $t_B = 1/4\pi$ (as solutions of the Hopf equation) and produce a stationary shock at $x = 0.5$. Two cases are shown: If $x = 0.5$ is a node x_n, then oscillations occur for $t > t_B$; if $x = 0.5$ is a half-node $x_{n+1/2}$, then no oscillations are generated. We explain this behavior and derive supplementary shock conditions of the form (3.18), with $\alpha = 0, 1, \infty$ for the initial data considered. This derivation depends only on the fact that the initial data are odd about the breaking point $x = 0.5$. In Section 4.2 we compare the results of Section 4.1 with exact solutions of the modulation equations for step and cubic root initial data—which have the same oddness property about the breaking point as the sine. We also discuss the occurrence of instabilities and finite time blowups in the solutions of (1.2) when the corresponding solutions of the modulation equations (3.4) satisfy the condition $ab > 0$ in (3.10), except at some point where ab and its derivative vanish. Finally, in Section 4.3 we present two numerical experiments exhibiting blowup as the modulation equations cross the elliptic boundary. A *local asymptotic description of the blowup is shown*.

4.1. The emergence of period-two oscillations

Here we consider solutions of (1.2) with periodic boundary conditions

$$u_{n+N} = u_N, \tag{4.2}$$

for some large N. For the initial data we take

$$u_n(0) = \sin(2\pi x_n), \qquad x_n = nh, \tag{4.3}$$

where $h = 1/N$ (note then that, in (1.3), $x_0 = 0$).

Clearly, we need to integrate only for $1 \le n \le N$, and we can restrict our attention to the interval $0 \le x \le 1$. We note the solution to the corresponding problem for the Hopf equation (1.1) is smooth for $0 \le t < 1/(4\pi) = t_B$ and develops a stationary shock at $x = 0.5$ for $t > t_B \approx 0.796$.

We show here the results of two calculations. One in Figure 1 with $N = 1000$ and the other in Figure 2 with $N = 1001$. The results are strikingly different. In Figure 1 we see period-two oscillations[28] arising at $x = 0.5$ at time $t \approx t_B$ and fanning out in both directions—to fill a region of width $\Delta x = O(t - t_B)$, centered at $x = 0.5$. A shock, in the sense of Sections 2.4 and 3.3 is clearly visible at $x = 0.5$. In contrast, no oscillations develop in Figure 2, and the solution corresponds to that of (1.1), even after $t = t_B$, with a steady shock in u at $x = 0.5$. The behavior in Figure 1h is addressed in Remark 4.4.

Note: Actually, two small bursts of oscillation (easily seen in the figures, as they move away from $x = 0.5$ on each side) are generated roughly at the time the shock forms in Figure 2. These bursts, however, vanish as $h \to 0$. As far as we can tell from our numerical experiments (carried for the values of $N = 1001$, 2001, 4001, and 8001), if a_b denotes the amplitude of these bursts then $h \ll a_b \ll 1$ as h vanishes.

These two different behaviors are actually quite easy to understand in terms of the theory developed in Section 3. In the first case $N = 2M$ is even and $x_M = 0.5$ is a node on the grid. Clearly then we must have $u_{M+j} = -u_{M-j}$ for the solution of (1.2) with initial conditions as in (4.3). In particular $u_M \equiv 0$ and $u_{M-1} \equiv -u_{M+1}$. This is consistent with the modulation equations (3.4) with a shock at $x = 0.5$ satisfying (3.12) and the additional condition[29]

$$a_+ = a_- = 0. \tag{4.4}$$

That is, (3.18) applies with $\alpha = \infty$ (equivalent to $\alpha = 0$ by exchanging the roles of a and b). In terms of R and S [see (3.11)], this translates into [30]

$$R = -S \quad \text{at } x = 0.5. \tag{4.5}$$

Then, for $0 \le t \le t_B$, one has $R = S = 0 = b_+ = b_-$ at $x = 0.5$ and no oscillations arise. For $t > t_B$ characteristics that bring $R > 0$ arrive at $x = 0.5$. Then $b_- = -b_+ > 0$ occurs there and oscillations develop. These are then carried away from $x = 0.5$ by S—note that binary oscillations occur if and only if $S \neq 0$. The position of the leading characteristics (starting at $x = 0.5$, $t = t_B$ and moving away to each side of $x = 0.5$) carrying the front of the oscillatory region $S \neq 0$ is very clear and sharply defined in the numerical calculations

[28] Because of the large number of points used it is impossible to distinguish individual oscillations in most of the figures (but, see Figure 1c). A direct inspection of the numerical output, however, shows this to be clearly the case—with, typically, $u_{n+2} - u_n = O(h)$. One envelope in the figures corresponds then to u_n for n even and the other to u_n for n odd.

[29] Note that in our calculations M is even, so that u_M corresponds to a by (3.1) and (3.3). For M odd, we must replace a by b in (4.4).

[30] We do not use the subscripts $+/-$ for R and S at the shock because (from their definition in (3.11) and the condition (3.12)) they are both continuous there.

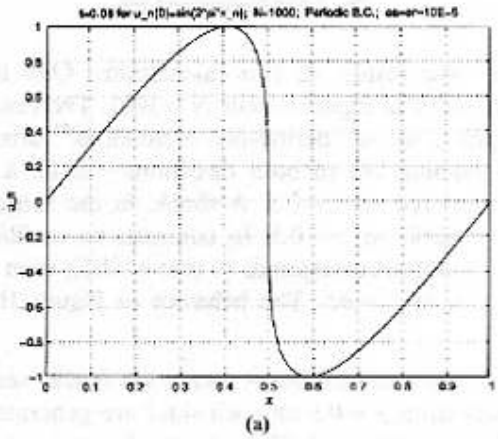

(a)

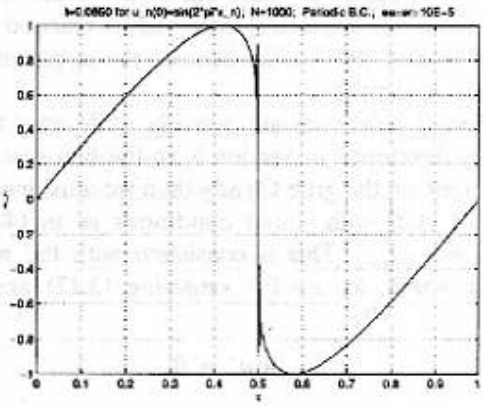

(b)

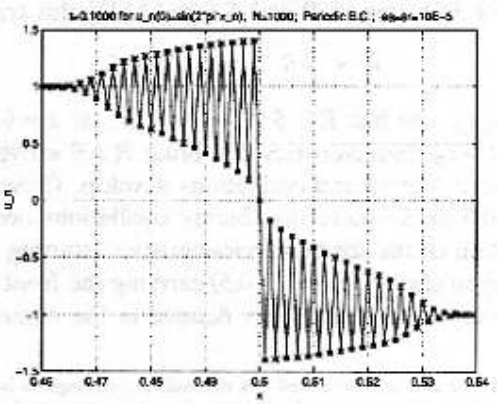

(c)

Figure 1. Solution of the scheme (1.2) with periodic boundary conditions and initial conditions $u_n(0) = \sin(2\pi x_n)$, where $0 \le x_n - nh \le 1$, $h = 1/N$, and $N = 1000$. u_n is shown for $t = 0.080$(a), 0.085(b), 0.120(d), 0.140(e), 0.150(f), 0.160(g), and 0.170(h). (c) Detail (in $0.46 \le x_n \le 0.54$) for $t = 0.100$, clearly showing binary oscillations. (h) Breakdown of the binary oscillations once $ab < 0$.

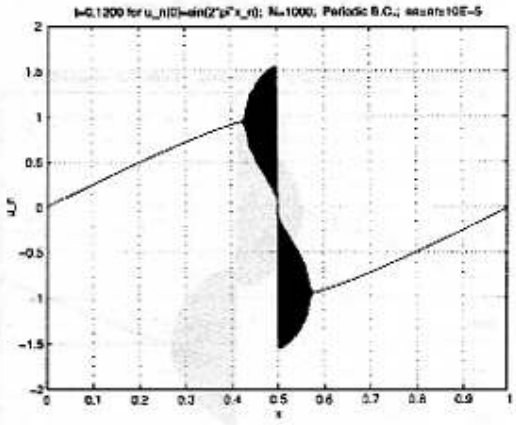

(d)

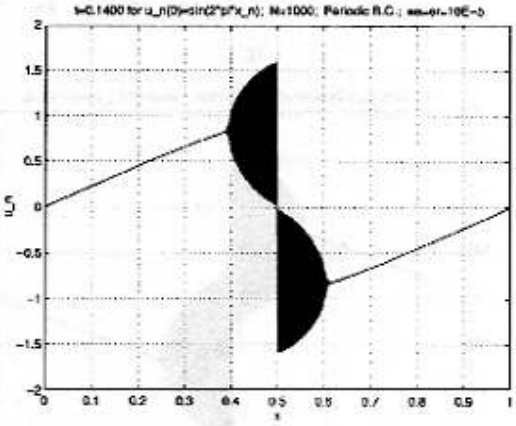

(e)

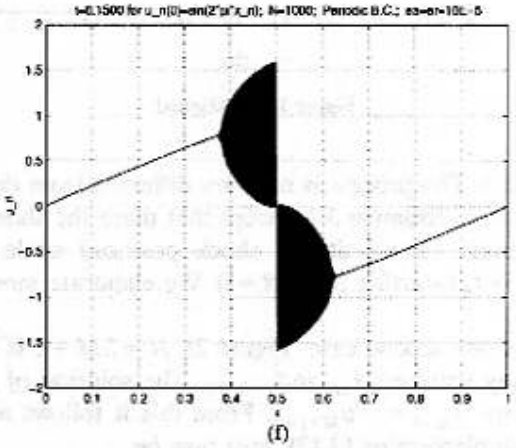

(f)

Figure 1. Continued.

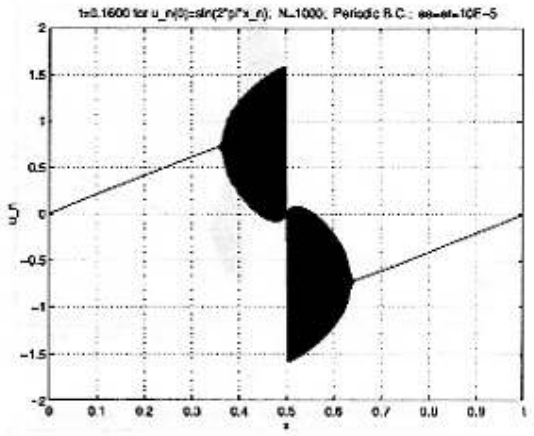

(g)

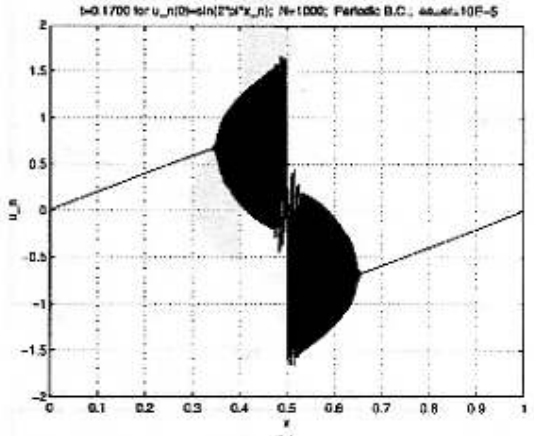

(h)

Figure 1. Continued.

shown in Figure 1. The process is not very different from that illustrated by the exact solution in Example 3.1, except that there the shock starts at $t = 0$ with finite strength ($R \equiv 2$ at the shock position) while here R grows gradually (for $t > t_B$) starting from $R = 0$. We elaborate more on this in the next subsection.

In contrast, in the second case (Figure 2), $N = 2M + 1$ is odd and $x = 0.5$ is exactly halfway between x_M and x_{M+1}. The solution of (1.2)–(4.3) then has the symmetry $u_{M-j} = -u_{M+j+1}$. From this it follows immediately that the condition supplementing (3.12) must now be

$$a_+ = -b_- \qquad \text{and} \qquad a_- = -b_+. \tag{4.6}$$

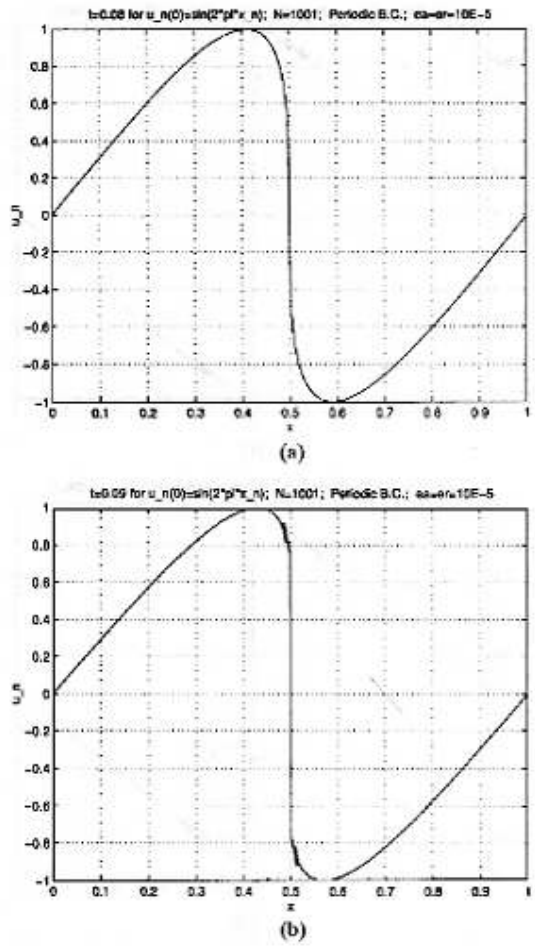

Figure 2. Solution of the scheme (1.2) with periodic boundary conditions and initial conditions $u_n(0) = \sin(2\pi x_n)$, where $0 \le x_n = nh \le 1$, $h = 1/N$, and $N = 1001$. (**a**-**d**) u_n is shown for $t = 0.08$(**a**), 0.09(**b**), 0.14(**c**), and 0.16(**d**). Small (of amplitude a_b, say) bursts of oscillations are generated when the shock forms. Their amplitudes vanish as $h \to 0$, but slowly: Various numerical calculations suggest $h \ll a_b \ll 1$.

Thus $a_+ = b_+ = -a_- = -b_-$, i.e., $\alpha = 1$ in (3.18). Obviously, no oscillations develop and the solution of the modulation equations (3.4) will have $a = b = U$, with a stationary shock at $x = 0.5$, as observed.

4.2. *Comparisons with exact solutions*

Here we compare the behavior occurring in the experiment of Figure 1 with some exact solutions of the binary modulation equations (3.4), with a shock satisfying (3.12) and (3.18) for $\alpha = 0$. First, in Figure 3, we show a plot of the

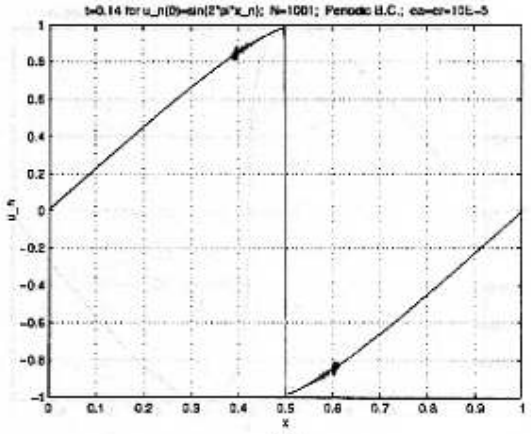

(c)

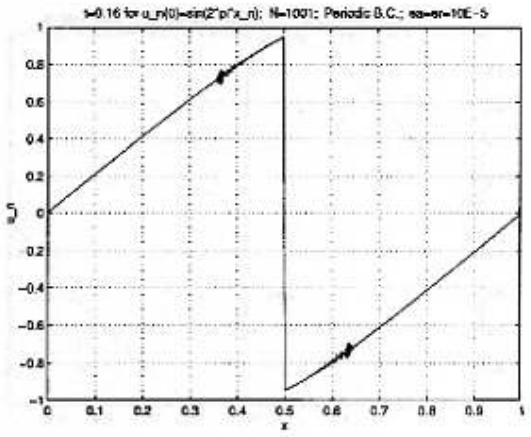

(d)

Figure 2. Continued.

solution of Example 3.1 for the case when $\alpha = 0$ in (3.13)—using (3.1) and (3.3) to recover u_n for $h = 0.001$ and $t = 0.1$. Note that, since it is a similarity solution, one plot is enough.

Remark 4.1: The most noticeable difference between the figures is in the behavior, at the shock, of the derivatives of a and b. In Figure 3 they vanish, while in Figure 1 they do not. This has to do with the fact that in one case the shock builds up strength slowly, starting from zero, and in the other case it does not.

Remark 4.2: The fact that in Figure 3 (exact solution of Example 3.1 for $\alpha = 0$) a and b have vanishing derivatives at the shock—with one of them

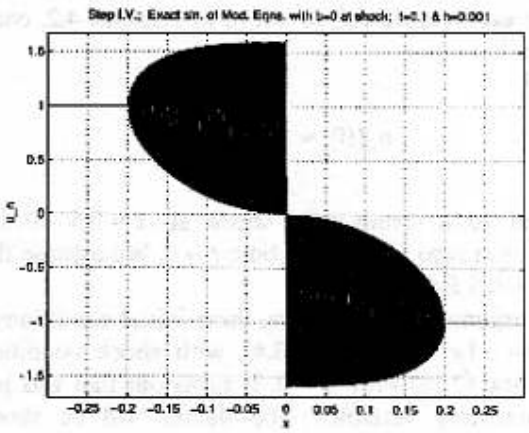

Figure 3. Exact solution of the modulation equations with symmetric (odd) step initial values, as in Example 3.1 for $\alpha = 0$. Using the asymptotic expansion in Section 3.1, u_n has been reconstructed for $t = 0.1$, $x_n = nh$, and $h = 0.001$. Here the function a is the envelope having a jump at $x = 0$ while the function b is the other envelope, vanishing at $x = 0$.

vanishing also—means that the solution remains very close to the elliptic boundary $ab = 0$ (see (3.10)) in some interval near the shock. This has serious implications concerning the applicability of this solution as a description of a corresponding solution for the scheme (1.2). For example, consider the initial data

$$u_n(0) = 1 \text{ for } n < 0 \qquad u_0(0) = 0, \qquad u_n(0) = -1 \text{ for } n > 0. \quad (4.7)$$

Then, as in the analysis before the solution of (4.3) with N even, symmetry arguments show that $u_n = -u_{-n}$ should apply for all times. Thus a shock in the modulation equations (3.4) is predicted at $x = 0$, satisfying (3.12) and (4.4). So, we should obtain the solution in Figure 3. However, the modulation equations (3.4) describe the behavior of (1.2) only in the limit $h \to 0$. For any finite h, however small, discretization errors occur—see (3.3). It appears that these are enough to push the solution of (1.2)–(4.7) into the unstable, elliptic, regime and then *blowup in a finite time occurs*. More details are given in Section 4.3 and Figure 5, where we show the results of a numerical calculation with the initial data (4.7).

Remark 4.3: If in (4.7) we take either $u_0(0) = 1$ or $u_0(0) = -1$; then the initial conditions are an exact steady solution of the equations. This is, in fact, Example 3.1 with $\alpha = 1$ in (3.13). Locally (near the shock) this corresponds with the situation in Figure 2.

To avoid the problem described above in Remark 4.2, consider now the initial conditions[31]

$$u_n(0) = -\sqrt[3]{x_n - 0.5}, \tag{4.8}$$

that would lead to a steady-state shock at $x = 0.5$ in the solution of (1.1)—starting from zero strength at time $t = 0$. We assume that $x = 0.5$ is a node—i.e., $x_M = 0.5$ for some M.

By the same arguments used before, these initial conditions correspond to $a(x,0) = b(x,0) = -(x - 0.5)^{1/3}$ in (3.4), with shock conditions at $x = 0.5$ given by (3.12) and (3.18) with $\alpha = 0$. It turns out that this problem can be solved using similarity variables—the details will be shown in a later publication. In Figure 4 we show a comparison between the solution of the scheme (1.2) with the initial conditions (4.8) and the prediction of modulation theory; the agreement is remarkably good.

Remark 4.4: Regarding Remarks 4.1 and 4.2 and the possible blowup of the solutions of the scheme (1.2) (when the solutions of the associated modulation equations (3.4) get "too close" to the elliptic boundary $ab = 0$), in the solution with initial conditions (4.3), N even as in Figure 1: as time advances the derivatives of a and b at the shock decrease in absolute value. Eventually they get to be too small and the instability is triggered. We can see this starting to occur in Figure 1g, for $t = 0.16$. In Figure 1h, for $t = 0.17$, the solution of (1.2) can no longer be described by binary oscillations near $x = 0.5$. Soon thereafter the solution blows up near the shock at $x = 0.5$. The nature of this blowup is exactly the same as that seen in the experiments shown in Section 4.3.

4.3. The loss of hyperbolicity in binary oscillations

Here we illustrate, with two numerical experiments, what happens when a period-two oscillation evolves into the elliptic region in (3.10) at some location. In the first experiment we use data corresponding to (4.7) in Remark 4.2. Namely, for some large $N = 2M$ even, we take $h = 1/N, 0 \le x_n = nh \le 1$, and

$$u_n(0) = 1 \text{ for } 1 \le n < M, \qquad u_M = 0, \qquad u_n = -1 \text{ for } M < n < N. \tag{4.9}$$

[31] Note that $(-x^{1/3})$ is the typical leading-order approximation near the break point for solutions of (1.1) at the time of breaking.

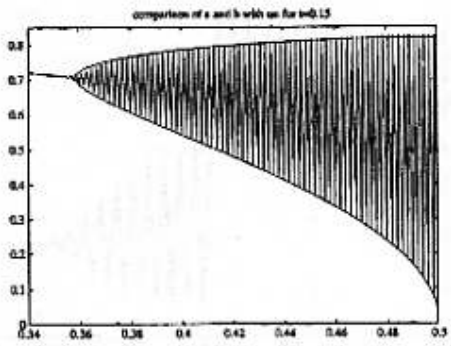

Figure 4. Solution of the scheme (1.2) for $t = 0.15$ in $0.34 \le x_n \le 0.5$ with initial conditions $u_n(0) = -\sqrt[3]{x_n - 0.5}$, $x_n = nh$, and $h = 1.001$. The drawn envelope is the corresponding exact solution of the modulation equations (3.4), with shock conditions given by (3.12) and (3.18) for $\alpha = 0$.

We use the boundary conditions $u_0 = 1 = -u_N$. The results, for $N = 1000$, appear in Figure 5. Initially period-two oscillations appear near $x = 0.5$ and fan out from this point in both directions as time increases. This is pretty much as the solution of Example 3.1 for $\alpha = 0$ would predict. Soon, however, the oscillation closest to $x = 0.5$ crosses into the elliptic region $ab < 0$, as explained in Remark 4.2. Explosive growth begins then there, and sometime around $t = 0.016$ and infinity seems to occur. Within the breakdown region (which is fairly narrow in space) the solution approaches a clear self-similar structure (see (4.11)), as seen in Figures 5g and 5h.

For a second experiment in Figure 6, we replace (4.9) by

$$u_n(0) = 1 - 2x_n, \qquad 1 \le n < N, \tag{4.10}$$

and keep everything else unchanged. In this case the Hopf equation should apply for $0 \le t < 0.25$, with a finite strength shock forming at $t = 0.25$. After that the solution of Example 3.1 for $\alpha = 0$ should apply (same as in the first experiment). The first part of this prediction holds true fairly well. However, after the shock forms at $t = 0.25$, the process described for the first experiment occurs faster, in about half the time as before—by $t = 0.258$ the blowup is clear.

Remark 4.5: Why should the blowup occur faster in this second experiment? We offer the following explanation: The solution for the Hopf equation in this case ($0 \le t < 0.25$) includes corners. As long as these corners are not too steep, (1.2) has no problem in approximating them. As the breakdown time approaches, however, the corners become very sharp. Close to these sharp corners then errors develop (one can see small "spikes"

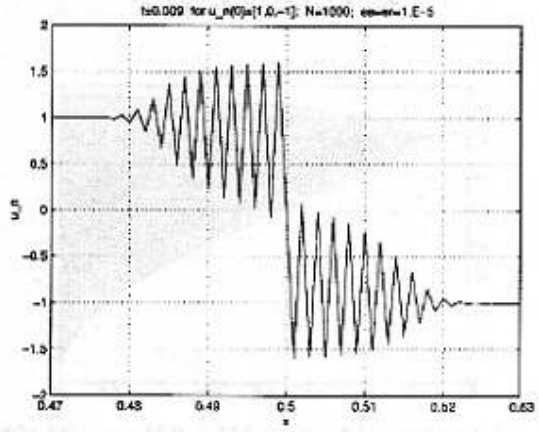

(a)

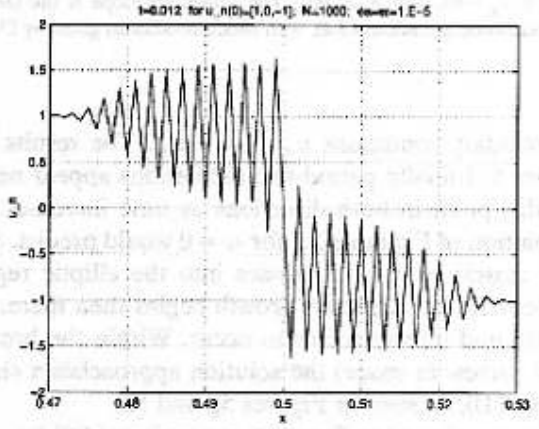

(b)

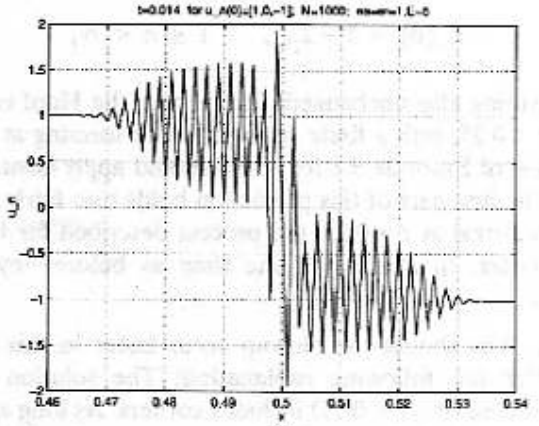

(c)

Figure 5. Solution of the scheme (1.2) with step initial data: $u_n = 1$ for $x_n < 0.5$, $u_n = -1$ for $x_n > 0.5$ and $u_{n=0} = 0$, where $x_n = nh$ and $h = 0.001$. u_n is shown in $0.47 \le x_n \le 0.53$ for $t = 0.009$(a) and 0.012(b). u_n is shown in $0.46 < x_n \le 0.54$ for $t = 0.014$(c), 0.015(d), 0.01557(e), and 0.015572(f). Details of the blowup are shown for $t = 0.01557$(g) and 0.015572(h) in $0.49 < x_n \le 0.51$.

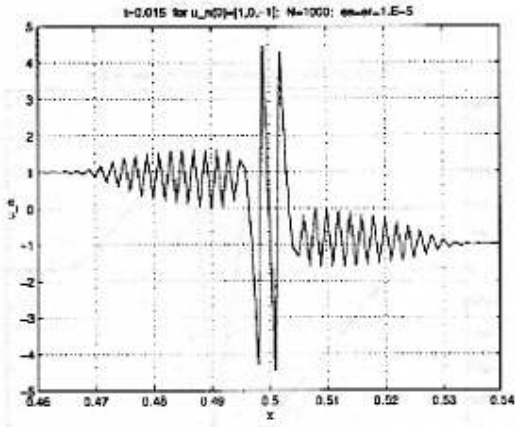

(d)

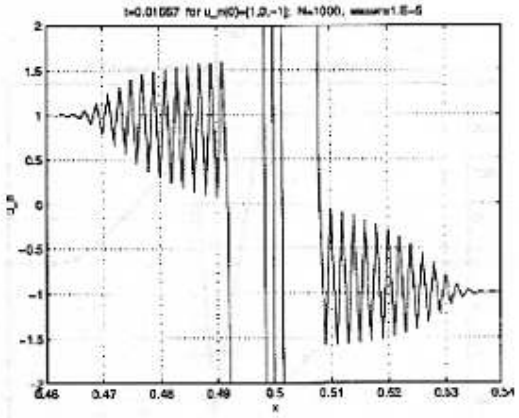

(e)

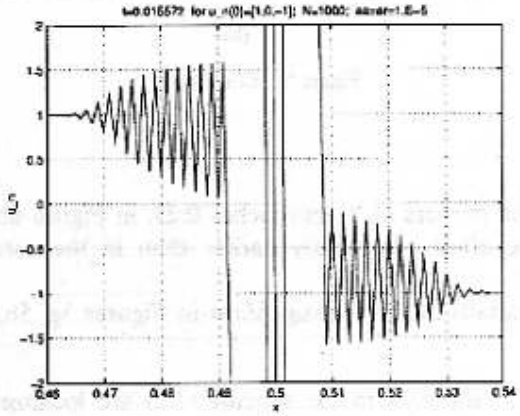

(f)

Figure 5. Continued.

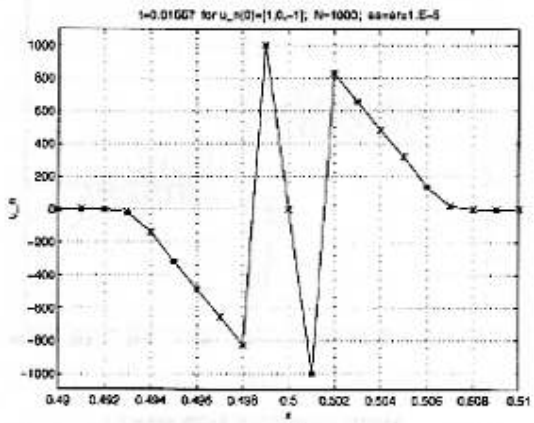

(g)

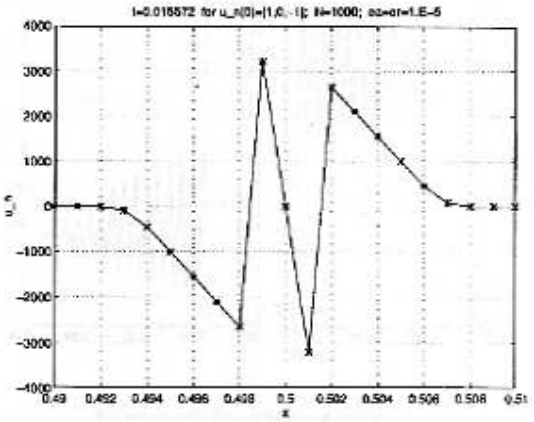

(h)

Figure 5. Continued.

forming near the corners as t approaches 0.25, in Figure 6b). These errors then trigger the elliptic instability earlier than in the case of the initial conditions (4.9).

Finally, the details of the blowup, show in Figures 5g, 5h, and 6f suggest the following

Conjecture 4.1: Blowups in the scheme (1.2) are localized in space and self-similar in time. If the blowup occurs near[32] $n = 0$, then as the time of

[32] Note that the equations are "translationally invariant," thus there is no loss of generality here.

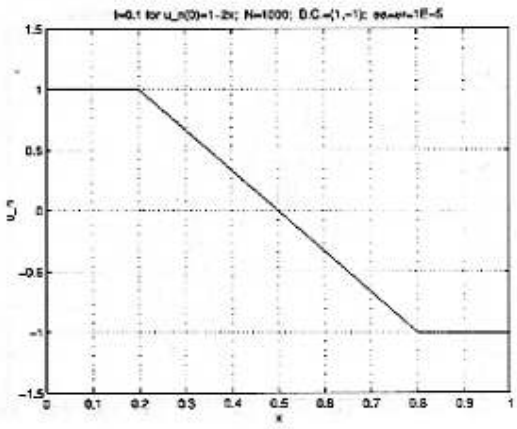

(a)

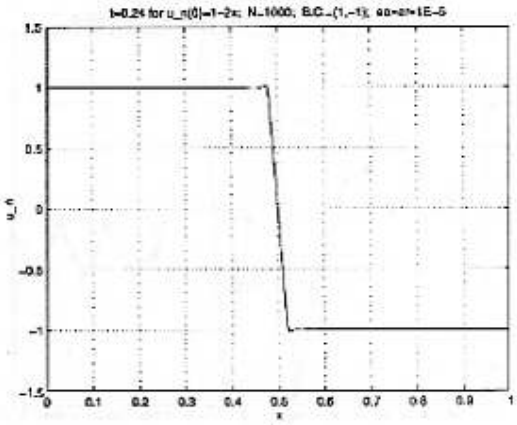

(b)

Figure 6. Solution of the scheme (1.2) with initial data $u_n(0) = 1 - 2x_n$ in $0 \le x_n = nh < 1$ with $h = 0.001$ and boundary conditions $u_0 = -u_{1000} = 1$. $t = 0.1$(a) and 0.24(b). Details of the oscillations and the blowup are shown in $0.49 \le x_n \le 0.51$ for $t = 0.253$(c), 0.2575(d), 0.2579(e), and 0.25803(f).

singularity t_s is approached ($0 < t_s - t \ll 1$) the solution near[33] $n = 0$ can be described by the following exact solution of (1.2),

$$u_n = \frac{h}{2}\left(\frac{\mu - n}{t_s - t}\right) \qquad \text{for } n \ge 2,$$

$$u_1 = -\frac{h}{2}\left(\frac{\mu - 1}{t_s - t}\right),$$

[33] Where "near" appears to mean $-6 \le n \le 6$.

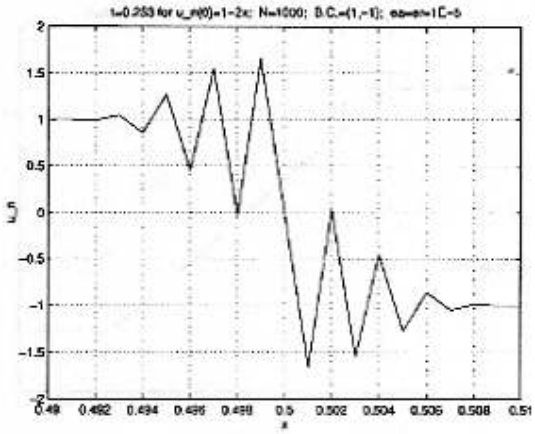

(c)

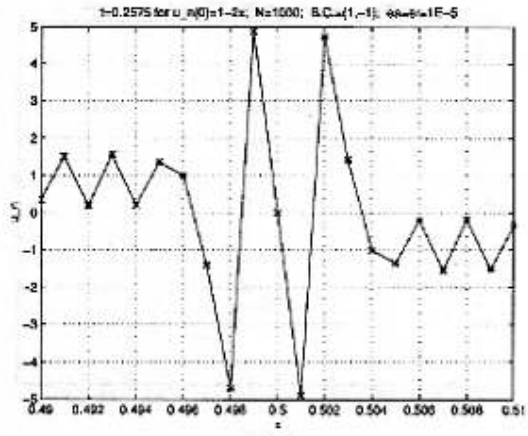

(d)

Figure 6. Continued.

$$u_0 = 0, \tag{4.11}$$

$$u_{-1} = \frac{h}{2}\left(\frac{\mu - 1}{t_s - t}\right),$$

$$u_n = -\frac{h}{2}\left(\frac{\mu + n}{t_s - t}\right) \qquad \text{for } n \leq -2,$$

where $\mu = 4 + 2\sqrt{2} \approx 6.83$. A straightforward calculation shows that this is a solution. The value of μ, which is uniquely determined for a solution of the form above, is the one that gives the narrow range of the blowup (which must occur between the zeros, at $\pm\mu$, of the solution).

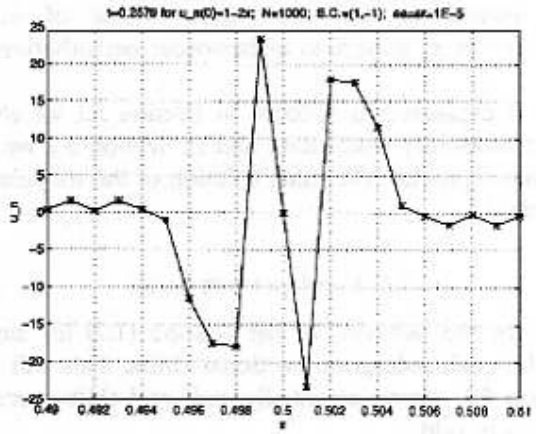

(e)

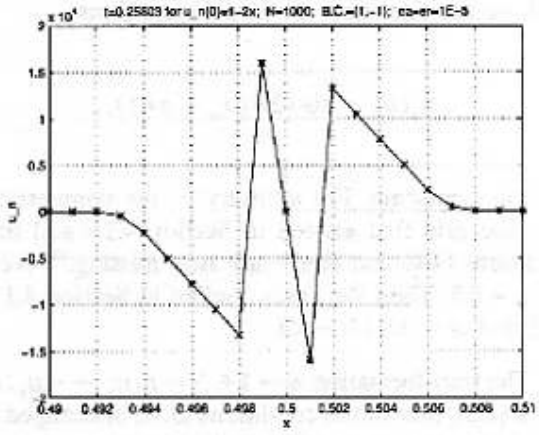

(f)

Figure 6. Continued.

5. Phase dependence in binary oscillations

In this section we investigate in some detail the *strong phase dependence* the solutions of the problem (1.2)–(1.3) can have in the limit $h \to 0$. From a theoretical point of view this dependence is related to the fact that the leading-order modulation equations for binary oscillations leave a "parameter" undetermined (see Remarks 3.4 and 3.6), which must therefore be sensitive to higher-order corrections:[34] Note that in (1.3) we can expand f in

[34] In fact, in a later publication, we show that the additional condition needed to complete (3.12) involves a coupling with second-order quantities.

Taylor series around x_n for some fixed choice of x_0; then small variations—$O(h)$—in x_0 appear as higher-order perturbations to the initial data.

This section is organized as follows: In Section 5.1 we study the phase dependence for sinusoidal initial data and in Section 5.2 we look at initial data for (1.2) that reproduce the exact solution of the modulation equations given in Example 3.1.

5.1. Envelopes with bellies

Here we illustrate the behavior of the scheme (1.2) for sinusoidal initial conditions as the grid undergoes fractional shifts. This will generalize the results in Section 4.1, where, essentially, half grid shifts were implemented by taking N even or odd.

For $h = 1/N, 1 \le n \le N, 0 < x_n = nh \le 1$, and periodic boundary conditions as in (4.2), we consider now the initial conditions

$$u_n(0) = \sin(2\pi(x_n - \sigma h)), \tag{5.1}$$

where $0 \le \sigma \le 1$ is a constant. For arbitrary σ, the symmetries of the initial data relative to the grid that existed in Section 4.1—and that we used to derive the conditions (4.4) and (4.6)—are now missing.[35] We take $N = 2M$ even, so that $x_M = 0.5$. Then the cases studied in Section 4.1 correspond to $\sigma = 0$ (N even) and $\sigma = 0.5$ (N odd).

Remark 5.1: The transformation $n \to 1 + N - n, u_n \to -u_n$, and $\sigma \to 1 - \sigma$ keeps the system (1.2), with initial conditions (5.1), unchanged. Thus, without loss of generality, we may assume $0 \le \sigma \le 1/2$.

The results of these experiments for $\sigma = 0.1$, 0.2, 0.3, and 0.4, $N = 2000$ and $t = 0.16$ are shown in Figure 7. The evolution of the solutions prior to the displayed time is as follows: For $0 < t < t_B$, the Hopf equation provides a good description. At $t \approx t_B$ and afterward, binary oscillations originate[36] near $x = 0.5$ and fan out in both directions from this point. *The amplitude of the oscillations generated, however, depends strongly on* σ.

If we model the condition at the shock in the binary oscillations present at $x = 0.5$ by (3.12) and (3.18), then $\alpha = \alpha(\sigma)$. From the symmetry arguments in Section 4.1 we know that $\alpha(0) = 0$ (will produce the maximum amplitude oscillations) and $\alpha(0.5) = 1$ (no oscillations). For other values of σ

[35] The location of the stationary shock generated by (5.1) in the Hopf equation is now at $x = 0.5 + \sigma h$. The breakdown time is still $t_B = 1/4\pi$.

[36] Except, for $\sigma = 0.5$, when the Hopf equation describes the solution for all times.

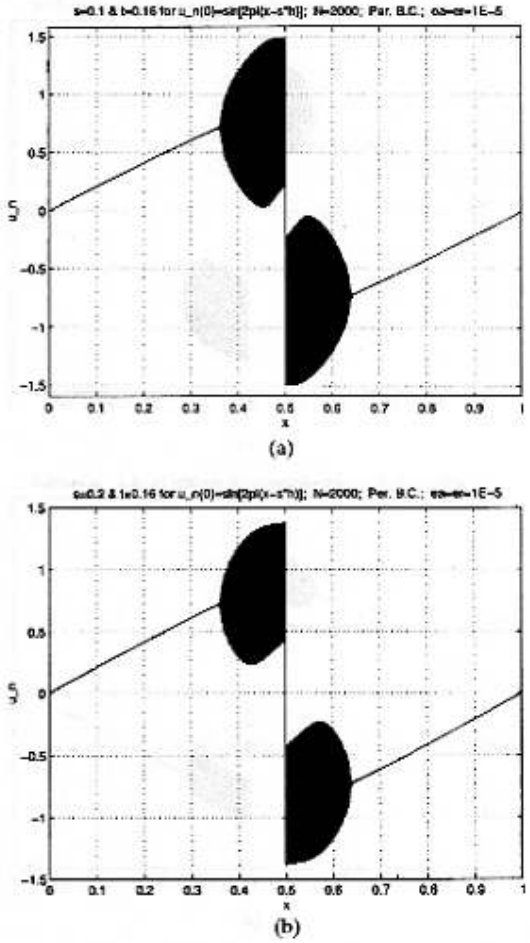

Figure 7. Solutions of the scheme (1.2) with periodic boundary conditions and initial data $u_0(0) = \sin(2\pi(x_n - \sigma h))$, where $0 \le x_n = nh < 1$, $h = 1/N$, $N = 2000$, and σ is a constant. u_n is displayed for $t = 0.16$ and (a)$\sigma = 0.1$, (b)$\sigma = 0.2$, (c)$\sigma = 0.3$, and (d)$\sigma = 0.4$. The edges of the shaded region represent the values of u_n for n even and odd (respectively).

we measured α from our numerical experiments and found the values:

$$\begin{aligned} \alpha(0.1) &\approx 0.14, \qquad \alpha(0.2) \approx 0.31, \\ \alpha(0.3) &\approx 0.46, \qquad \alpha(0.4) \approx 0.71. \end{aligned} \tag{5.2}$$

Of course, (3.18) is only exactly valid for $\sigma = 0$ and $\sigma = 0.5$. For other values of σ the correct condition is subtler and will be studied in a later publica-

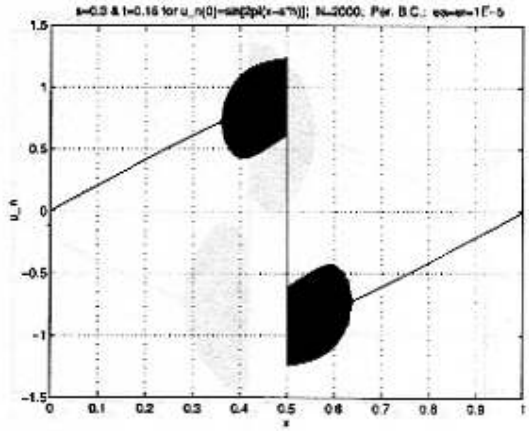

(c)

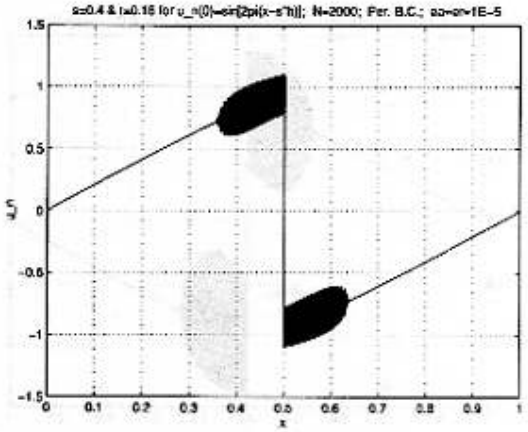

(d)

Figure 7. Continued.

tion. Nevertheless, the ad hoc condition (3.18) has the correct qualitative properties, and if used to numerically integrate the modulation equations (with the values in (5.2)) it produces results that agree with those shown in Figure 7.

Remark 5.2: We note that, in several of the graphs in Figure 7 the envelope closer to the x axis has a "belly." As time advances the belly grows and eventually reaches the x axis. At the point of contact, the hyperbolicity condition $ab > 0$ (see (3.10)) ceases to apply, the period-two solutions become unstable, and exactly the same type of blowup described in Section 4.3 is triggered.

5.2. *Comparisons with exact solutions*

In view of the results of Section 5.1, it would be interesting to design initial conditions for the scheme (1.2) that yield solutions that can be compared with the exact ones found in Example 3.1 for values of α not 0 or 1. This turns out to be fairly easy: Consider a shifted version of the second experiment in Section 4.3. Namely, take

$$u_n(0) = \begin{cases} 1 & \text{for } x_n \le 0.5 - \rho + \sigma h, \\ -(1/\rho)(x - 0.5 - \sigma h) & \text{for } |x_n - 0.5 - \sigma h| \le \rho, \\ -1 & \text{for } x_n \ge 0.5 + \rho + \sigma h, \end{cases} \tag{5.3}$$

where $0 < \rho < 0.5$ is a constant, $1 \le n < N$, $h = 1/N$, $x_n = nh$, N is large and even,[37] and σ is the shift parameter, $0 \le \sigma \le 0.5$. The boundary conditions $u_0 = 1 = -u_N$ should be used. Just as in Section 5.1, for $0 < \sigma < 0.5$, there are no symmetries in the mesh relative to the initial data. Thus we expect values of α other than 0 or 1 to occur.

The solution of the Hopf equation corresponding to the data (5.3) breaks and forms a steady state of finite constant strength after $t = t_B = \rho/2$. Thereafter we expect binary oscillations that should correspond to the solution in Example 3.1 for some α in (3.13). In our calculations we took $\rho = 1/3$ and $N = 1000$. The results, for $\sigma = 0.2, 0.3$ and $= 0.24$ are displayed in Figure 8. The agreement with the predictions of Example 3.1 is quite good. For example, for $\sigma = 0.3$, the experiment corresponds to $\alpha \approx 0.48$ (this predicts values of a and b next to the shock of $a \approx 1.3$ and $b \approx 0.63$, as in the figure). Note that the values of α needed here are not too different from the ones we computed for sinusoidal initial data in (5.2).

Remark 5.3: When $\alpha > 0$, the solutions to the modulation equations stay well inside the hyperbolic region $ab > 0$ and blowups do not occur (see Remarks 4.4 and 4.5). However, the errors produced by the corner present in the solution of the Hopf equation with initial data corresponding to (5.3) still occur (see Remark 4.5). These errors seem to be the source of the small oscillations (which are not part of the exact solution in Example 3.1) that can be seen in the envelopes in Figure 8. These oscillations are stronger near the "heads" of the oscillatory regions and fade out near the shock as time advances. This, of course, is because the disturbance caused by the corners at the moment of shock formation moves away with the heads of the oscillatory regions.

[37] Thus $x = 0.5$ is a node: $x_M = 0.5$, where $N = 2M$.

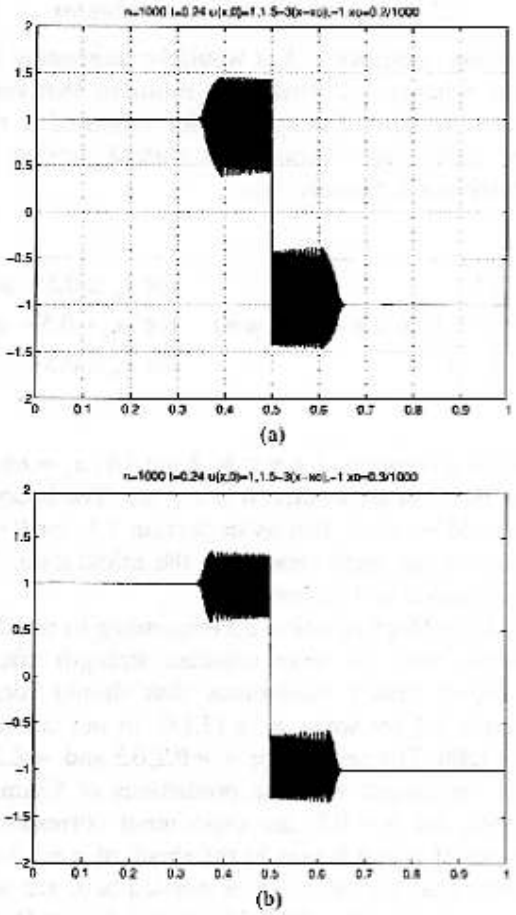

Figure 8. Solutions of the scheme (1.2) with boundary conditions $u_0 = 1$, $u_N = -1$ and initial data as in Equation (5.3), with $\rho = \frac{1}{3}$, $h = 1/N$, and $N = 1000$. The solution is displayed in $0 \le x_n = nh \le 1$ for $t = 0.24$ and $\sigma = 0.2$(a) and 0.3(b).

To avoid the difficulty pointed out in Remark 5.3 above, we also considered initial conditions of the form

$$u_n(0) = -\tanh[10(x_n - 0.5 - \sigma h)] \tag{5.4}$$

to replace (5.3). These should also settle into solutions of the sort found in Example 3.1, but (since now the process of shock formation is gradual) less "noise" should be produced when the shock is formed. On the other hand, the formation period of the shock is now not as Example 3.1 would have it, so the shapes of the envelopes near the heads of the waves will differ.

The results of the experiments with initial conditions as in (5.4) are presented in Figure 9, for $N = 1000$, $t = 0.2$ and $\sigma = 0$, 0.1, 0.2, and 0.3. Again, theoretical arguments show that $\alpha(0) = 0$ and $\alpha(0.5) = 1$. The following other values follow from the numerical data

$$\begin{aligned} &\alpha(0.1) \approx 0.148, \quad \alpha(0.2) \approx 0.308, \\ &\alpha(0.3) \approx 0.491, \quad \alpha(0.4) \approx 0.713. \end{aligned} \tag{5.5}$$

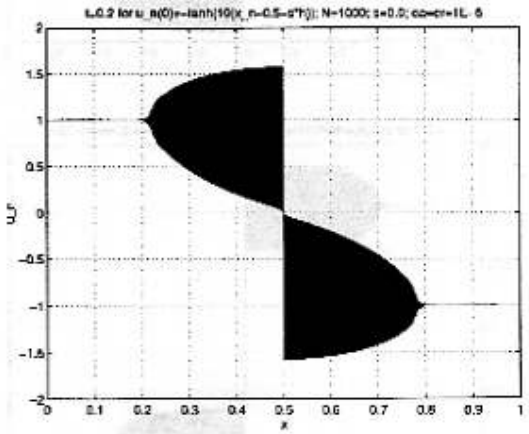

(a)

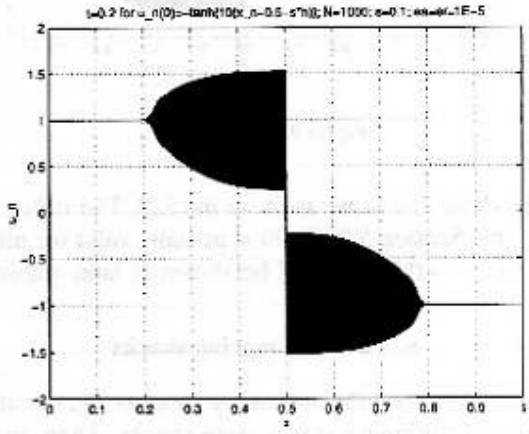

(b)

Figure 9. Solutions of the scheme (1.2) with boundary conditions: u_0 and u_N constant, and initial data: $u_n(0) = -\tanh(10(x_n + 0.5 - \sigma h))$, where $0 \le x_n = nh \le 1$, $h = 1/N$, $N = 1000$ and σ is a constant. u_n is displayed for $t = 0.2$ and $\sigma = 0.0$(a), 0.1(b), 0.2(c), and 0.3(d).

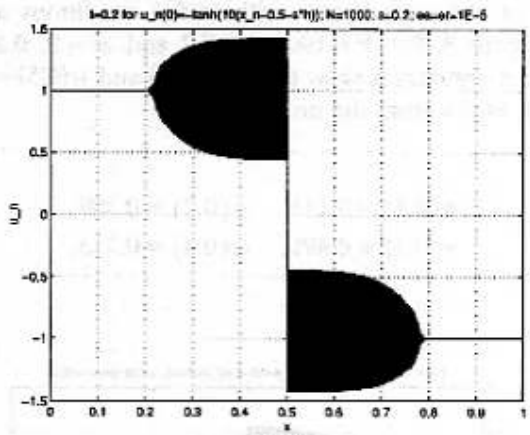

(c)

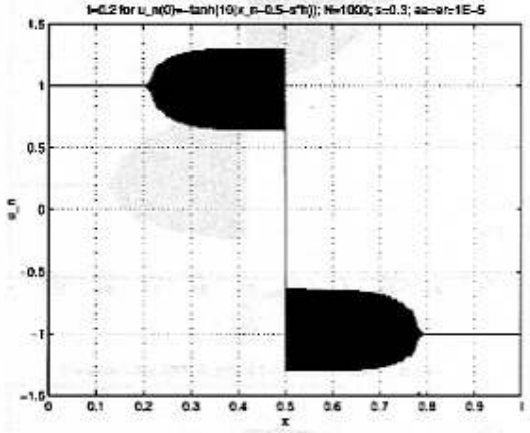

(d)

Figure 9. Continued.

These values are about the same as those in (5.2). The difference is that, for the examples in this Section 5.2, (3.18) is actually valid for all values[38] of σ, not just $\sigma = 0$ and $\sigma = 0.5$. This will be shown in later publication.

6. Pulses in moving shocks

In Section 3 we showed that the stationary modulation equations for binary oscillations admitted stationary steady-state shocks. Then, in Sections 4 and 5, we studied solutions of the scheme that exhibited these type of shocks.

[38] Thus it is possible, in particular, to measure the values of α with accuracy. In general, as we mentioned earlier, (3.18) is only a rough approximation to the true condition, so that α is not even defined accurately.

We showed that they have a very strong phase dependence—with the amount of oscillations generated varying from none (when the shock fell exactly halfway between nodes x_n) to the maximum allowed by the hyperbolicity condition $ab > 0$ (when the shock coincided with a node x_n).

Now a natural question is: What happens if initial conditions are given that are a small perturbation of those that give stationary shocks, as above? In particular, what happens when a shock moves (slowly) through the grid? We may speculate a priori that pulses of oscillation will be generated, achieving their maximums when the shock intersects a grid point and decreasing to a minimum in between intersections. These pulses will then move away from the location of the shock.

Of course, as the modulation equations for binary oscillations are hyperbolic and nonlinear, the shape of the pulses will distort in time—and different pulses may interact. This should lead to situations where the equations cease to be valid, What happens afterward is one of the main questions we would like to investigate. It appears worthwhile, therefore, to set up an experiment in which this situation arises. Thus consider the following set of initial conditions for (1.2)

$$u_n(0) = \delta + \sin 2\pi x_n, \qquad x_n = nh, \tag{6.1}$$

where δ is a small constant, as usual $h = 1/N$ and $1 \le n \le N$ for some large N, and we use periodic boundary conditions. The corresponding solution of the Hopf equation in this case breaks at $t_B = 1/4\pi \approx 0.0796$, $x_B = 2\delta t_B + 0.5$. Thereafter a shock forms that moves at speed 2δ.

The results of an experiment with $\delta = 0.01$ and $N = 4000$, with conditions as in (6.1), are shown in Figure 10. A pulse is indeed formed each time the shock crosses a node—except that the shock speed is not 2δ, but somewhere in the range 2.2δ to 2.3δ. The first pulse formed[39] is clearly binary in nature when it forms; later ones are not but are almost so. We make the following observations.

(a) The characteristic speed[40] $\lambda = 2\sqrt{ab}$ is maximal when $a = b$, i.e., when there are no oscillations. Thus the pulses tend to steepen from the "back," a feature clearly visible in the figures. Wave breakdown failure of the binary modulation equations should eventually occur.

(b) Successive pulses do not move at the same speed. In fact, as a pulse moves away from the shock it slows down.[41] In consequence, the pulses tend to "pile up" as time progresses. As they interact more and more, the departures from a simple binary oscillation model become larger and larger.

[39] This requires close inspection of the output. It is not clear from the figure.

[40] The pulses to the right of the shock move following, roughly, the characteristics with speed λ. Those to the left move with speed $-\lambda$.

[41] A (not very accurate) explanation is that the pulses "ride" on a mean level that is decreasing. Thus, so does their overall speed.

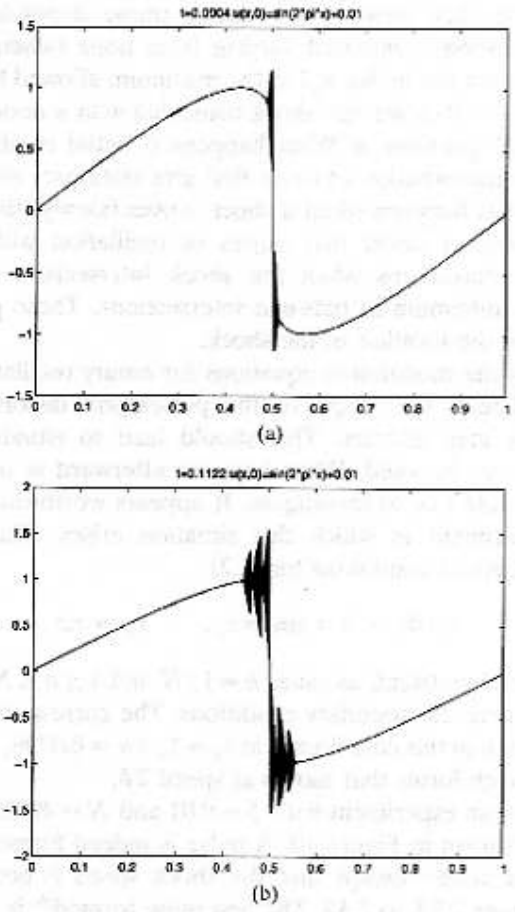

Figure 10. Solution of the scheme (1.2) with periodic boundary conditions and initial data $u_n(0) = 0.01 + \sin(2\pi x_n)$, where $0 \le x_n - nh < 1$, $h = 1/N$ and $N = 4000$. u_n is displayed for $t = 0.0904$(a), 0.1122(b), 0.1231(c), and 0.1500(d). (d) Pulses have already started to merge and interact.

A more detailed analysis of the behavior of slowly moving shocks of the type above—and the pulses they generate—will be presented in a later publication.

Finally, we point out that when δ in (6.1) is not small, as the shock in the Hopf equations forms, the oscillations that arise in the solution of the scheme are not period two and appear to be quite complicated. An example of this is shown in Figure 11, for $\delta = 0.5$ and $N = 1000$. If the oscillations shown in this experiment were binary, Figure 11b ($M = 1$ average in (4.1))

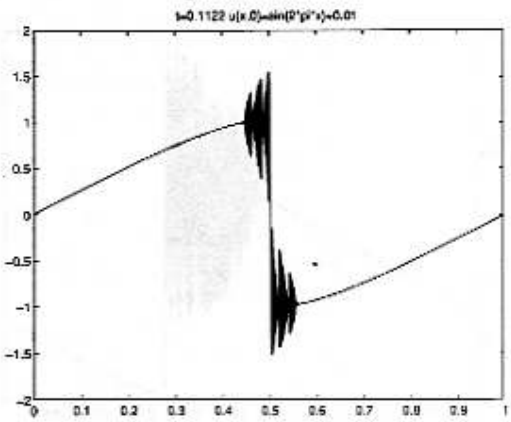

(c)

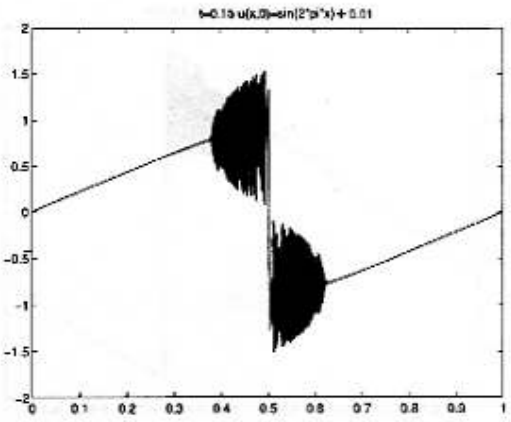

(d)

Figure 10. Continued.

would show no oscillations. This figure shows that, even though there is a large binary component in the solution, that is not all (by a wide margin).

Acknowledgments

The work of Cristina Turner was partially sponsored by grants from CONICOR (Project No. 2882/93), CONICET (Project No. 0551/92), and SECYT-UNC (Project No. 89). During 1989–1990 she had a CONICET scholarship (Beca Externa de CONICET). A visit to MIT during November 1992 was partially supported by the Sloan Foundation and NSF Grant DMS-

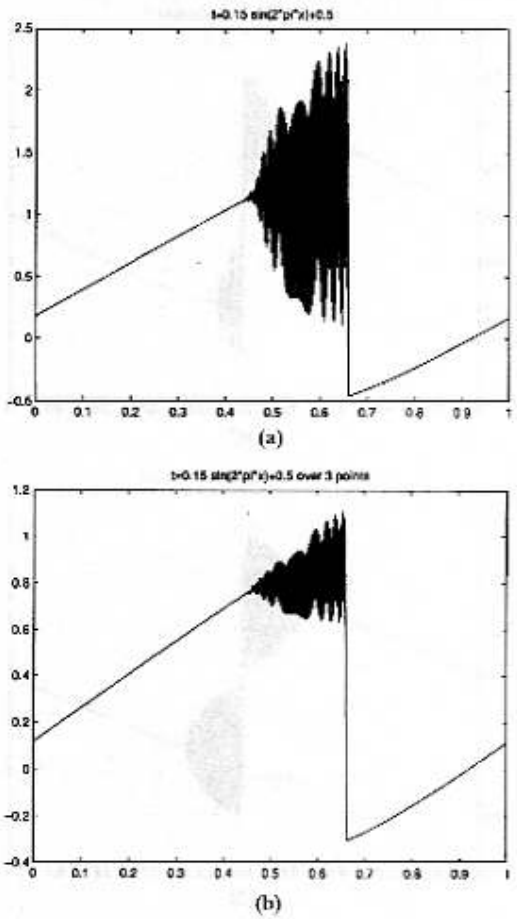

Figure 11. Solution of the scheme (1.2) with periodic boundary conditions and initial data $u_n(0) = 0.5 + \sin(2\pi x_n)$, where $0 \le x_n - nh \le 1$, $h = 1/N$, and $N = 1000$. (a) u_n is displayed for $t = 0.15$. Equation (4.1) averages of this solution for $M = 1$(b) and $M = 15$(c). Clearly, the oscillations are not binary.

9008520. Her research at MSRI during the first semester of 1994 was supported in part by NSF Grant DMS 90221140. The first author thanks Esteban Tabak for his comments and encouragement during the course of this research and Peter Lax, Percy Deift, David Levermore, Jonathan Goodman, and Stephanos Venakides for their questions and helpful advice during her stay at MSRI. The work of Rodolfo R. Rosales was partially supported by NSF Grants DMS-9008520, INT-9016555, and DMS-9311438. He also acknowledges the support of the University of Córdoba (FaMAF) during his visits there.

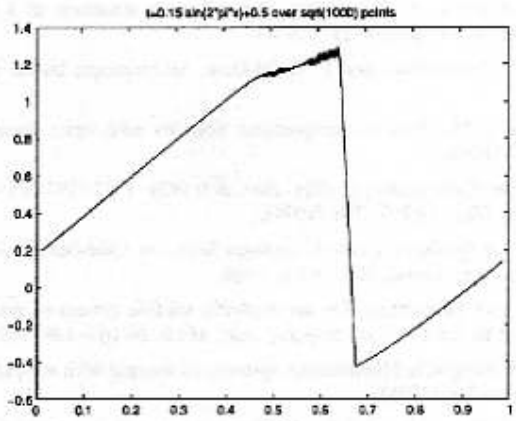

(c)

Figure 11. Continued.

References

1. P. D. Lax and C. D. Levermore, The zero dispersion limit of the Korteweg–de Vries equation, *Proc. Natl. Acad. Sci. USA* 76(8):3602–3606 (1979); The small dispersion limit of the Korteweg–de Vries equation, I, II, III, *Comm. Pure Appl. Math.* 36:253–290, 571–593, 809–829 (resp.) (1983).
2. S. Venakides, The zero dispersion limit of the Korteweg–de Vries equation with nontrivial reflection coefficient, *Comm. Pure Appl. Math.* 38:125–155 (1985); The generation of modulated wave trains in the solution of the Korteweg–de Vries equation, *Comm. Pure Appl. Math.* 38:883–909 (1985); The zero dispersion limit of the Korteweg–de Vries equation with periodic initial data, *AMS Trans.* 301:189–225 (1987); The continuum limit of theta functions, *Comm. Pure Appl. Math.* 42:711–728 (1989); Higher order Lax–Levermore theory, *Comm. Pure Appl. Math.* 43:335–362 (1990).
3. P. D. Lax, C. D. Levermore, and S. Venakides, The generation and propagation of oscillations in dispersive IVPs and their limiting behavior, in *Important Developments in Soliton Theory* 1980–1990 (T. Fokas and V. E. Zakharov, Eds.), pp. 205–241, Springer Verlag, Berlin, 1992.
4. G. Strang, Accurate partial differential methods, II, *Numer. Math.* 6:37–46 (1964).
5. G. B. Whitham, *Linear and Nonlinear Waves*, Wiley, New York, 1974.
6. D. W. McLaughlin and J. Strain, Calculating the weak limit of KdV by quadratic programming, in *Singular Limits of Dispersive Waves*, (N. Ercolani, I. Gabitov, D. Levermore, and D. Serre, Eds.), NATO ARW Series B320, Plenum, New York, 1994.
7. F. R. Tian, Oscillations of the zero dispersion limit of the Korteweg–de Vries equation, *Comm. Pure Appl. Math.* 46:1093–1129 (1993).
8. O. C. Wright, Korteweg–de Vries Zero Dispersion Limit: A Restricted Initial Value Problem, Ph.D. dissertation, Princeton University, 1991.
9. H. Flaschka, M. G. Forest, and D. W. McLaughlin, Multiple phase averaging and the inverse spectral solution of the Korteweg–de Vries equation, *Comm. Pure Appl. Math.* 33:739–784 (1980).
10. M. J. Ablowitz and H. Segur, *Solitons and the Inverse Spectral Transform*, SIAM, Philadelphia, 1981.

11. A. V. Gurevich and L. P. Pitaevskii, Nonstationary structure of a collisionless shock wave, *Soviet Phys. JETP* 38:291–297 (1974).

12. M. Hays, C. D. Levermore, and P. D. Miller, Macroscopic lattice dynamics, *Phys. D* 79:1–15 (1994).

13. P. Rosenau and J. M. Hyman, Compactons: Solitons with finite wavelength, *Phys. Rev. Lett.* 70:564–567 (1993).

14. H. Flaschka, The Toda lattice, I, *Phys. Rev. B* 9:1924–1925 (1974); On the Toda lattice, II, *Prog. Theoret. Phys.* 51:703–716, (1974).

15. M. Toda, *Theory of Nonlinear Lattices*, Springer Series in Solid-State Sciences, Vol. 20, 2nd enlarged ed., Springer Verlag, New York, 1988.

16. M. Kac and P. van Moerbeke, On an explicitly soluble system of nonlinear differential equations related to certain Toda lattices, *Adv. Math.* 16:160–169 (1975).

17. J. Moser, Three integrable Hamiltonian systems connected with isospectral deformations, *Adv. Math.* 16:197–220 (1975).

18. B. L. Holian, H. Flaschka, and D. W. McLaughlin, Shock waves in the Toda lattice: Analysis, *Phys. Rev. A* 24:2595–2623 (1981).

19. S. Venakides, P. Deift, and R. Oba, The Toda shock problem, *Comm. Pure Appl. Math.* 44:1171–1242 (1990).

20. J. Goodman and P. D. Lax, On dispersive difference schemes, I, *Comm. Pure Appl. Math.* 41:591–613 (1988).

21. B. T. Hayes, Binary modulated oscillations in a semi-discrete version of Burgers equation, *Phys. D*, in press (1997).

22. T. Y. Hou and P. D. Lax, Dispersive approximations in fluid dynamics, *Comm. Pure Appl. Math.* 44:1–40 (1991).

23. C. D. Levermore and J.-G. Liu, Large oscillations arising in a dispersive numerical scheme, *Physica D*, 99:191–216 (1996). Oscillations arising in numerical experiments, in *Singular Limits of Dispersive Waves* (N. Ercolani, I. Gabitov, D. Levermore, and D. Serre, Eds.), NATO ARW Series B320, pp. 329–346, Plenum, New York, 1994.

24. J. von Neumann, Proposal and analysis of a new numerical method in the treatment of hydrodynamical shock problems in *Collected Works. VI* Pergamon Press, New York, 1961.

25. E. Fermi, J. Pasta, and S. Ulam, Studies of Nonlinear Problems, Los Alamos Report LA-1940 (1955), in *Collected Papers of Enrico Fermi. II*, pp. 978–988 Univ. of Chicago Press, Chicago, 1965.

26. J. C. Bronski and D. W. McLaughlin, Semiclassical behavior in the NLS equation: Optical shocks-focusing instabilities, in *Singular Limits of Dispersive Waves* (N. Ercolani, I. Gabitov, D. Levermore, and D. Serre, Eds.), NATO ARW Series B320, Plenum, New York, 1994.

27. S. Jin, C. D. Levermore, and D. W. McLaughlin, The behavior of solutions of the NLS equation in the semiclassical limit, in *Singular Limits of Dispersive Waves* (N. Ercolani, I. Gabitov, D. Levermore, and D. Serre, Eds.), NATO ARW Series B320, pp. 335–355, Plenum, New York, 1994.

28. P. D. Lax, *Hyperbolic Systems of Conservation Laws and the Mathematical Theory of Shock Waves*, SIAM Regional Conference Series in Applied Mathematics, Vol. 11, 1973.

29. L. F. Shampine and M. K. Gordon, *Computer Solution of Ordinary Differential Equations*, W. H. Freeman, San Francisco, 1975.

Universidad Nacional de Córdoba
Massachusetts Institute of Technology

(Received April 25, 1995)